Autodesk®
Moldflow Insight
2019

Fiber Orientation Solver Validation

Several enhancements and improvements were implemented in Autodesk Moldflow Insight (AMI) 2019, including (1) the new *Intermediate fiber orientation tensor* result, (2) the improvement of automatic parameters in Moldflow Rotational Diffusion (MRD) model, and (3) the fountain flow effect on fiber orientation prediction. The fiber orientation predictions were validated against the measured fiber orientation data from a number of injection-molded parts, and the comparison demonstrates the improvement of the fiber orientation prediction over the previous release.

Contents

Introduction

Fiber orientation in injection-molded parts exhibits a typical core-shell-skin structure through the half-thickness, as illustrated in Figure 1. Near the midplane, the shearing is weak, and fibers are aligned randomly or transversely, depending on the flow condition near the gate. This region is called the core layer. Near the wall surfaces, the shearing is dominant, and fibers are strongly aligned in the flow direction. This is called the shell layer. In thin layers close to the surfaces, a weak alignment is normally observed, and this is due to the fountain flow which brings fibers with a weak alignment from the core to the wall surfaces [1, 2].

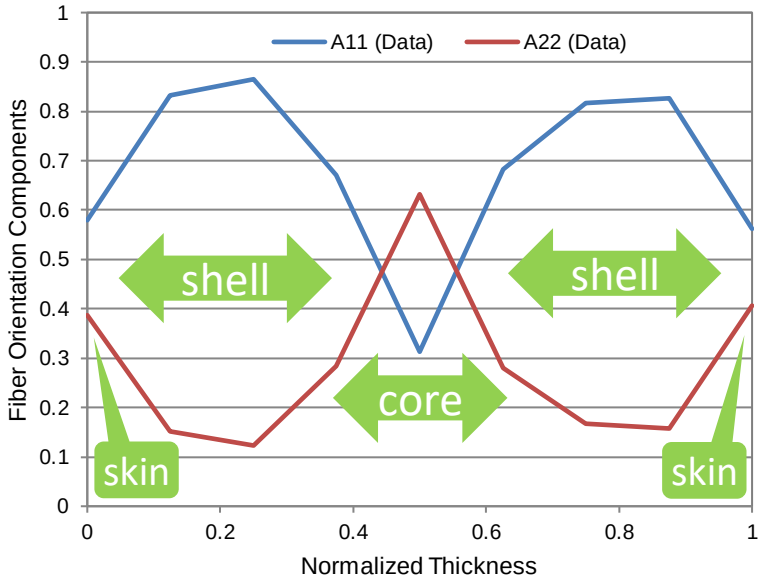

Figure 1. Typical orientation structure through the thickness in measured fiber orientation data of an injection-molded part.

A new intermediate fiber result has been added in AMI 2019 to help better understand the fiber orientation behavior during the injection molding process. Improvements have been implemented in AMI 2019 to achieve better fiber orientation predictions in the shell and skin regions.

Intermediate fiber orientation result

In the releases prior to AMI 2019, the fiber orientation result is only output at the end of analysis, and it can be used to study the effect of the fiber orientation on the mechanical properties and the warpage of the final part. In AMI 2019, an option was added to enable the output of the intermediate fiber orientation result at specified time intervals during the analysis. The intermediate fiber orientation result provides a tool to better understand the evolution of the fiber orientation during the filling and packing stages and to help users achieve better part designs and optimized processing conditions.

Figure 2 shows the new option of *Output intermediate fiber orientation results* in the *Fiber Solver Parameters* dialog box. This option is disabled by default, as the output of the intermediate fiber orientation result requires additional storage space and the size of the result file may increase significantly for some large models. The time step for the

intermediate result output is controlled by the constant intervals or specified times, as shown in Figures 3 and 4, for Midplane/Dual Domain and 3D models, respectively.

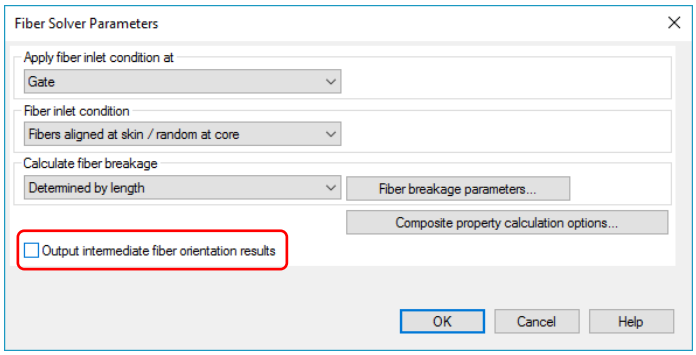

Figure 2. New option of *Output intermediate fiber orientation results* in *Fiber Solver Parameters* dialog box.

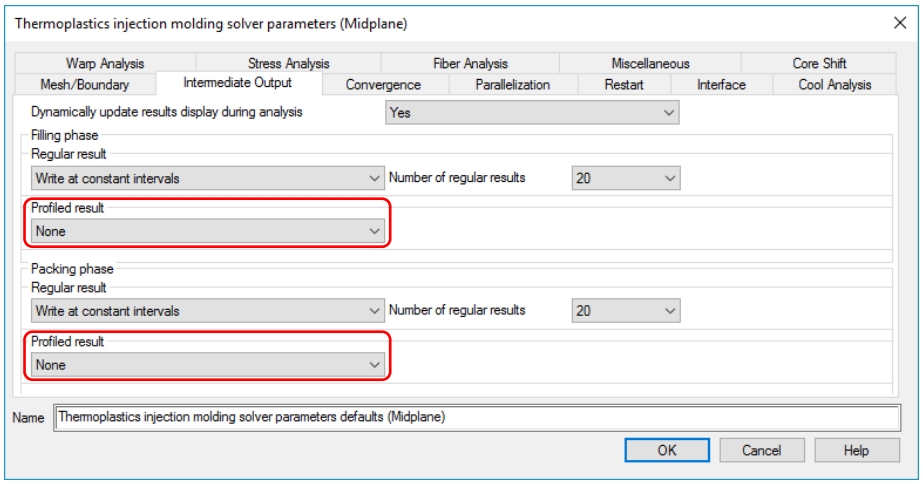

Figure 3. Option to specify time steps for intermediate result output and default values in *Process Settings* > *Advanced options* > *Solver parameters* dialog box for Midplane/Dual Domain model.

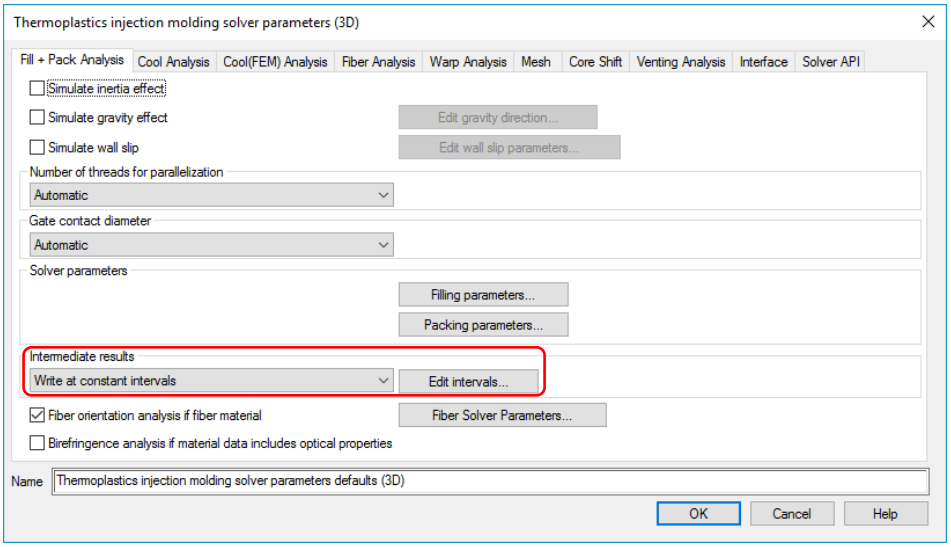

Figure 4. Option to specify time steps for intermediate result output and default value in *Process Settings* > *Advanced options* > *Solver parameters* dialog box for 3D model.

A new result named *Intermediate fiber orientation tensor* will be available in the result list when the *Output intermediate fiber orientation results* option is enabled and the time step for the intermediate result output is specified. The *Intermediate fiber orientation tensor* result is dependent on time and thickness for Midplane/Dual Domain and dependent on time for 3D model.

Moldflow Rotational Diffusion model parameters

The Moldflow Rotational Diffusion (MRD) model was introduced in AMI 2017R2 and is the default fiber orientation model for 3D models and short fiber materials. In AMI 2019, the automatically calculated parameters for the MRD model have been adjusted to better match measured fiber orientation data, and the default parameter values are: fiber interaction parameter C_I = 0.0015, and MRD parameters D_1 = 1, D_2 = 0.5, D_3 = 0.3.

A 3 mm thick end-gated plaque was injection-molded with Polypacific EXTRON 3019 HS (30%wt glass fiber-filled polypropylene). The part geometry and model mesh are illustrated in Figure 5. The fiber orientation was measured through the thickness at the center of the plaque, which was labeled as ROI1, and was compared with the fiber orientation predictions from AMI 2018.2 and AMI 2019 in Figure 6, in which A_{11} is the orientation component in the plaque length direction while A_{22} in the plaque width direction. Here the default MRD model and the default fiber parameters were used. Because of the more realistic fiber parameters, AMI 2019 predicts stronger fiber alignment in the part length direction and weaker aligner in the part width direction than AMI 2018.2 in shell layers (near the normalized thicknesses of 0.2 and 0.8), and AMI 2019 provides better agreement with experimental data than AMI 2018.2.

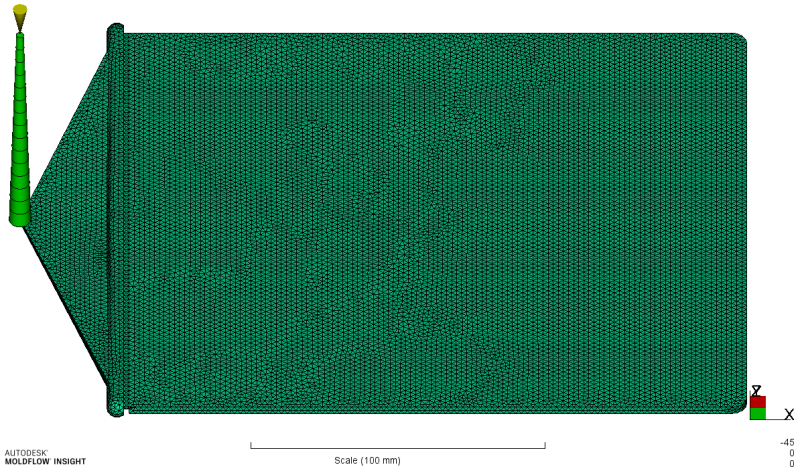

Figure 5. Geometry and 3D mesh of the mechanical plaque.

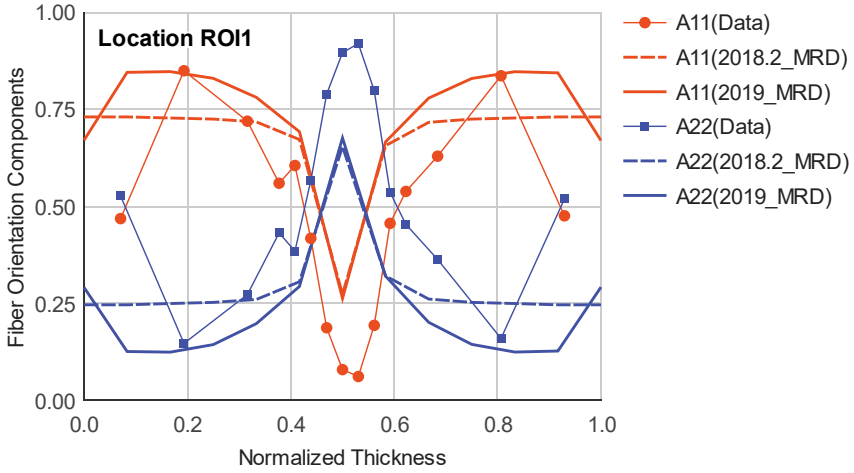

Figure 6. Comparison of fiber orientation data and predictions by AMI 2018.2 and AMI 2019 in the mechanical plaque.

Fountain flow effect on fiber orientation

In AMI 2019 the fountain flow has been considered for the fiber orientation prediction. For each wall node, the corresponding fountain flow location is found, and the fiber orientation of the fountain flow location is mapped to the wall node. This improvement changes the fiber orientation result of all the wall nodes, but its influence on internal results is small or negligible. The improvement also influences the warpage prediction.

Figure 7 compares the fiber orientation tensor results of the mechanical plaque in AMI 2018.2 and AMI 2019, and shows the significant difference as the plots display only the results on surfaces.

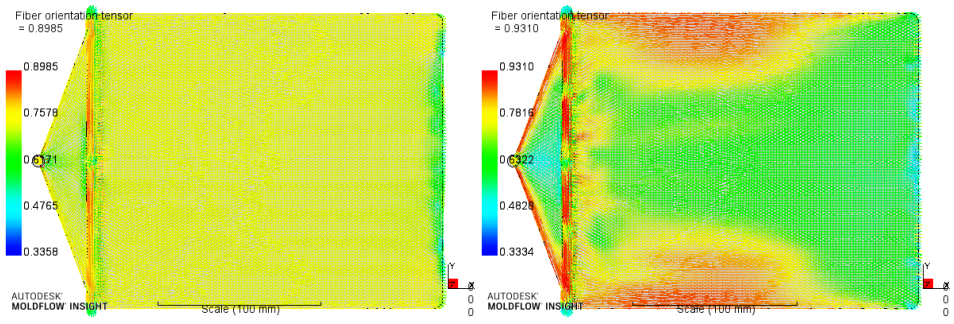

Figure 7. Fiber orientation results on surfaces of the mechanical plaque in AMI 2018.2 (left) and AMI 2019 (right).

The fiber orientation predictions in AMI 2018.2 and AMI 2019 are compared with the experimental data in Figure 6. Without the consideration of the fountain flow effect, AMI 2018.2 predicted almost uniform fiber orientation in the thickness near the surfaces. As the fountain flow effect on fiber orientation is taken into account, AMI 2019 produces a good agreement with the experimental data in the skin layers.

Validation of fiber orientation predictions

Delphi plaques and disks

A number of end-gated plaques and center-gated disks were molded with SABIC Innovative Plastics Valox 420-1001 (30 wt% glass fiber-reinforced polybutylene terephthalate) by Delphi Automotive LLP. The ISO-standard plaques were 80 mm wide and 90 mm long, and the disks were 90 mm in radius. The part thicknesses for each shape varied from 1.5, 2, 3, to 6 mm, and three different injection rates, referred to as slow, medium, and fast, were applied for each thickness [3].

Fiber orientation measurements were performed on three sections, each about 10 mm wide, starting at 0, 30, and 60 mm away from the gate on the cut along the centerline of each plaque, and along the radius of each disk. The sections are labeled as locations A, B, and C, respectively, as shown in Figure 8. For some parts, experimental data from location C are not available.

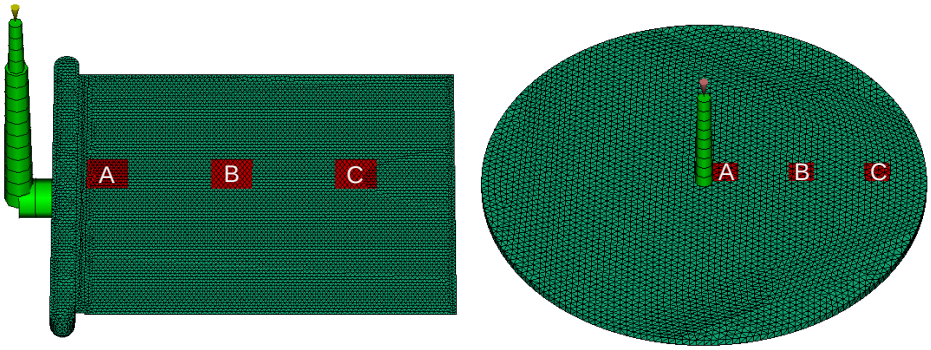

Figure 8. Geometry, 3D mesh, and locations of measurement samples for Delphi edge-gated plaque (left) and center-gated disk (right).

The fiber orientation predictions in AMI 2018.2 and AMI 2019 are compared with the experimental data in Figures 9 – 32. The predictions from both the Moldflow Rotary Diffusion (MRD) and the Reduced Strain Closure (RSC) models are displayed. Due to the improvement of the default model parameters of the MRD model, AMI 2019 provides better agreement with the experimental data in shell layers than AMI 2018.2, especially in the thin parts (1.5 and 2 mm thick) and at locations B and C. In the thick parts (3 and 6 mm thick) and at location A, fibers in shearing regions are not fully aligned, thus the shell orientation differences between AMI 2018.2 and AMI 2019 are small. Without the consideration of the fountain flow effect, AMI 2018.2 predicts almost uniform fiber orientation close the surfaces and is unable to match the skin orientation in most parts. AMI 2019 captures the weak fiber alignment in the skin orientation due to the fountain flow effect and produces better agreement with the experimental data than AMI 2018.2, for both the MRD and RSC models.

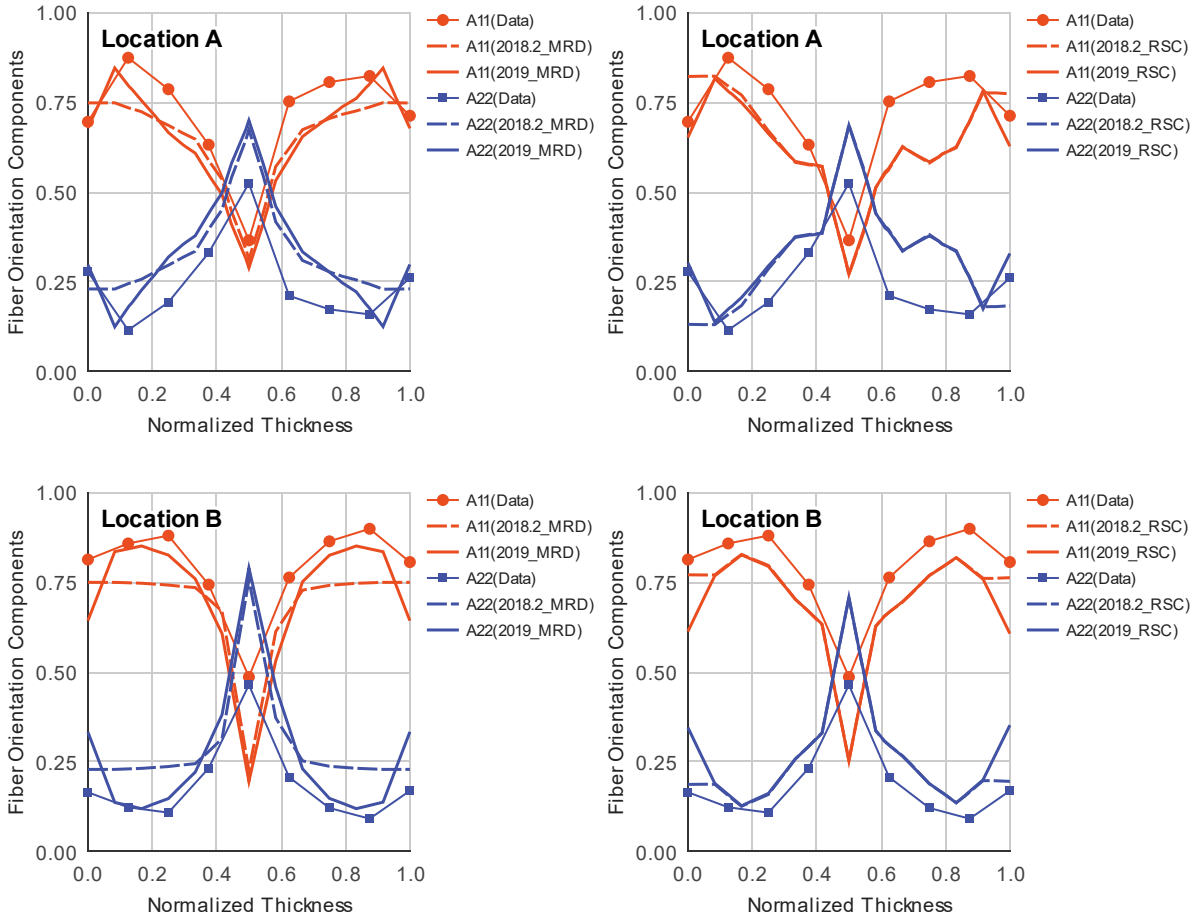

Figure 9. Comparison of fiber orientation data and MRD (left) and RSC (right) predictions by AMI 2018.2 and AMI 2019 in the Delphi ISO-standard plaque of 1.5 mm thick and slow fill rate.

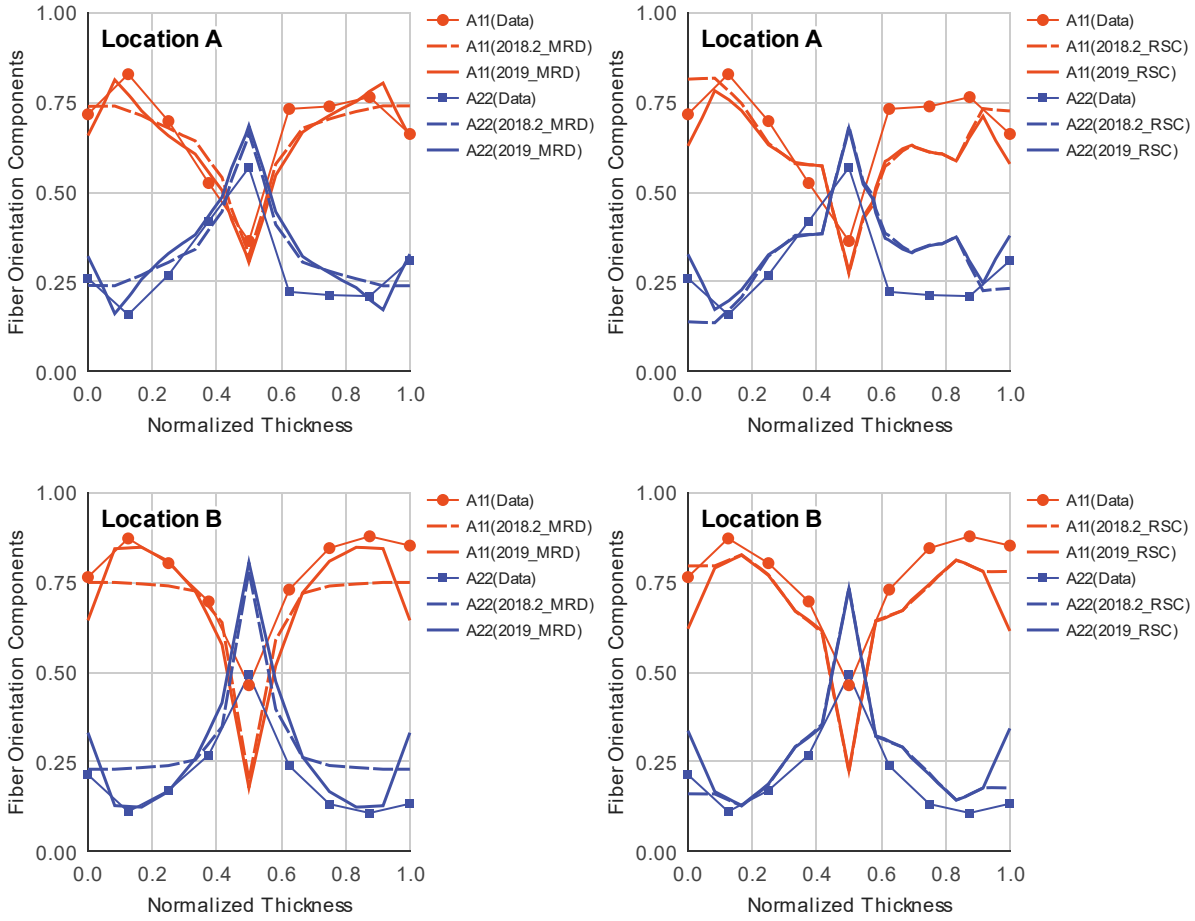

Figure 10. Comparison of fiber orientation data and MRD (left) and RSC (right) predictions by AMI 2018.2 and AMI 2019 in the Delphi ISO-standard plaque of 1.5 mm thick and medium fill rate.

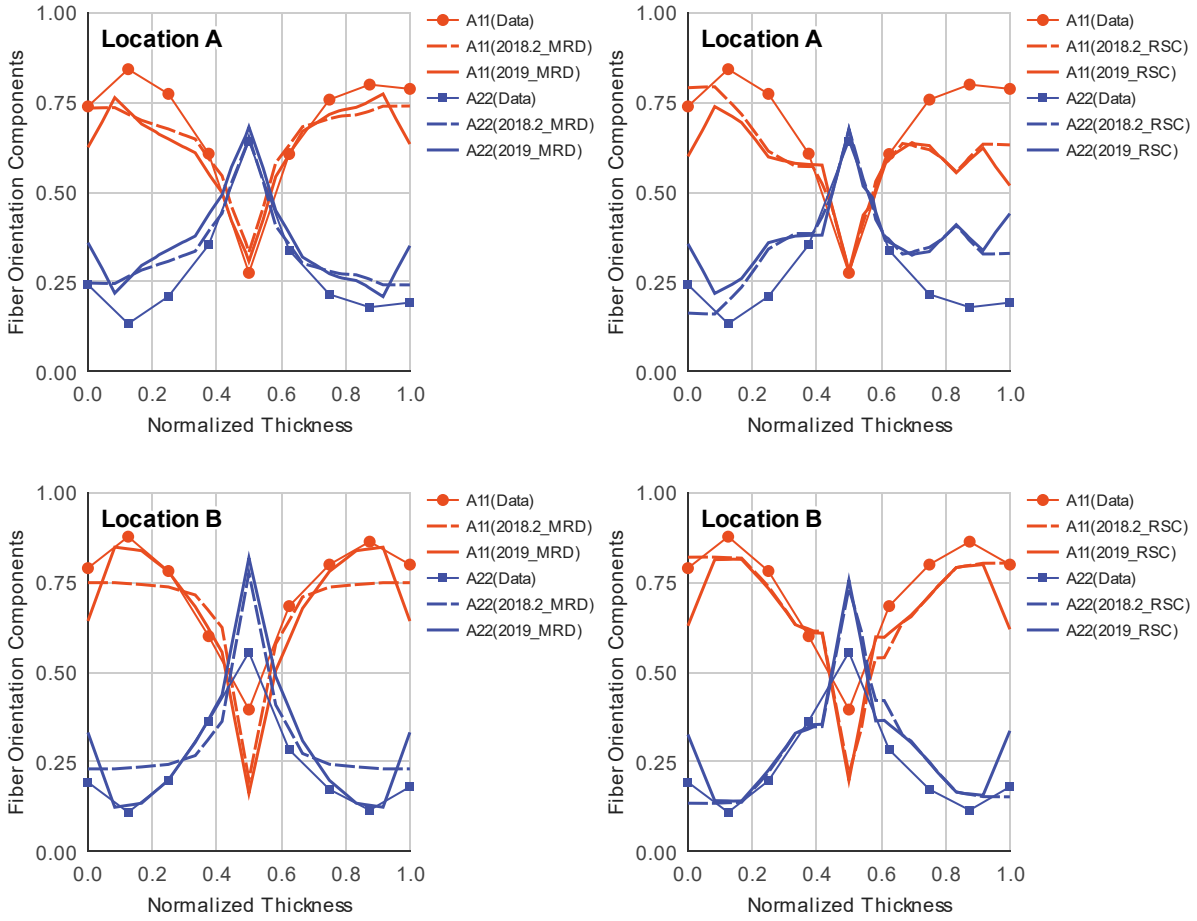

Figure 11. Comparison of fiber orientation data and MRD (left) and RSC (right) predictions by AMI 2018.2 and AMI 2019 in the Delphi ISO-standard plaque of 1.5 mm thick and fast fill rate.

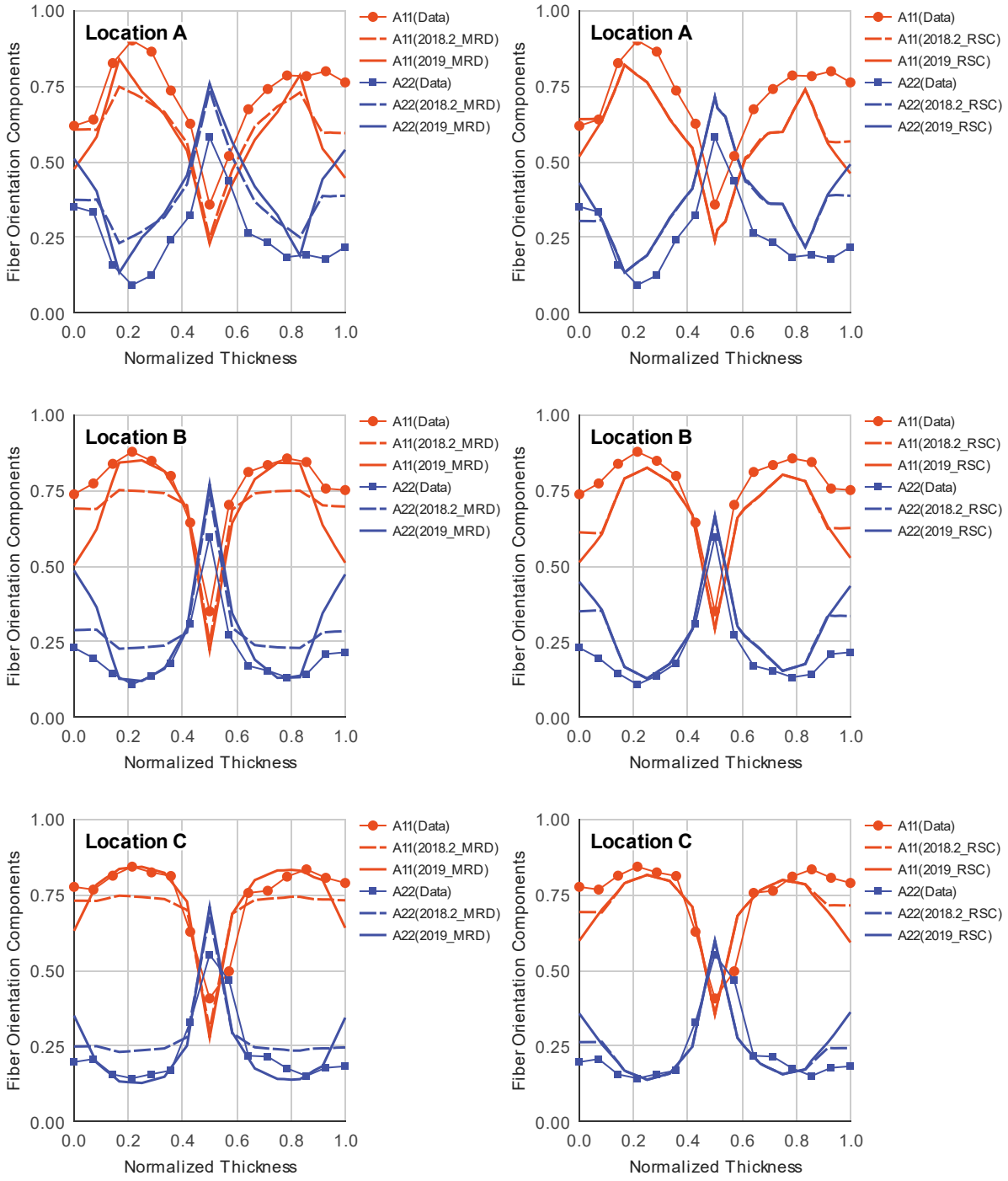

Figure 12. Comparison of fiber orientation data and MRD (left) and RSC (right) predictions by AMI 2018.2 and AMI 2019 in the Delphi ISO-standard plaque of 2 mm thick and slow fill rate.

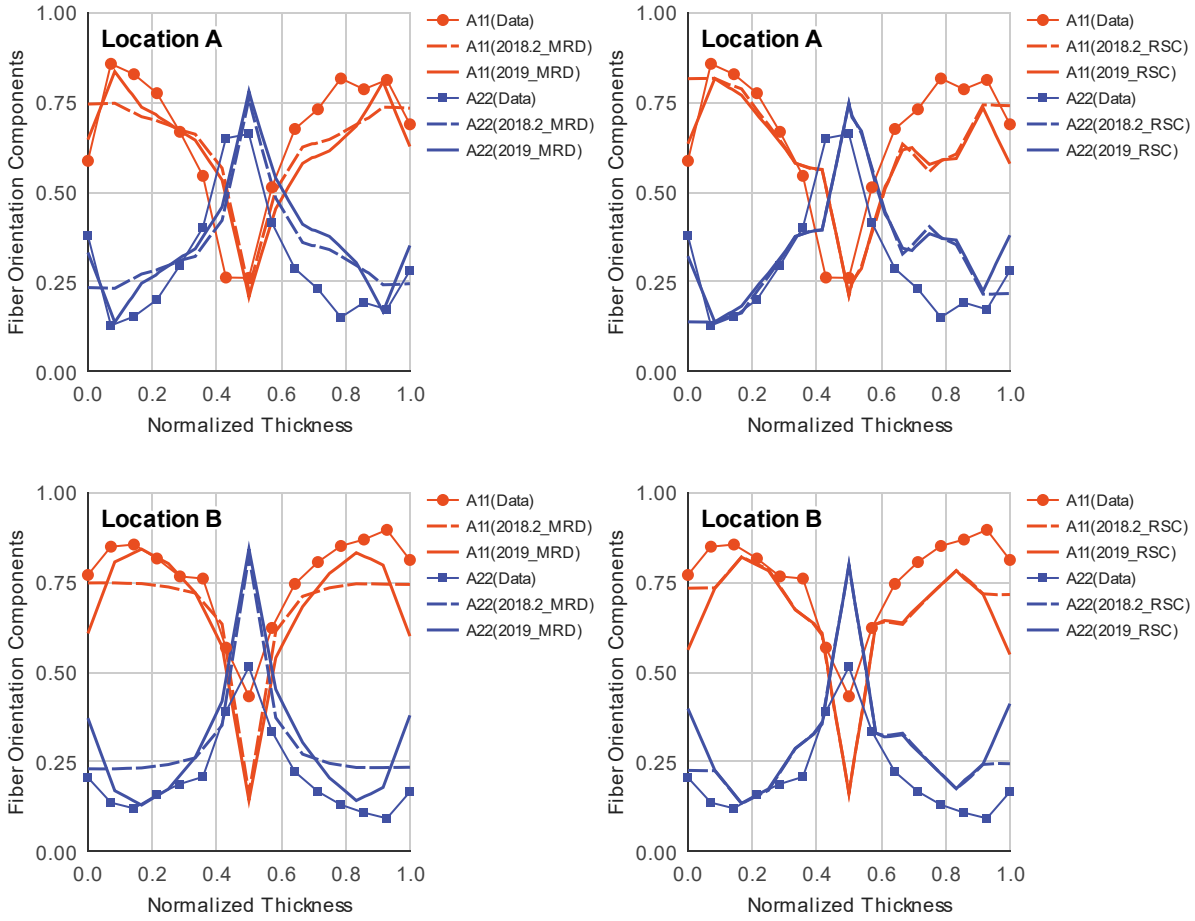

Figure 13. Comparison of fiber orientation data and MRD (left) and RSC (right) predictions by AMI 2018.2 and AMI 2019 in the Delphi ISO-standard plaque of 2 mm thick and medium fill rate.

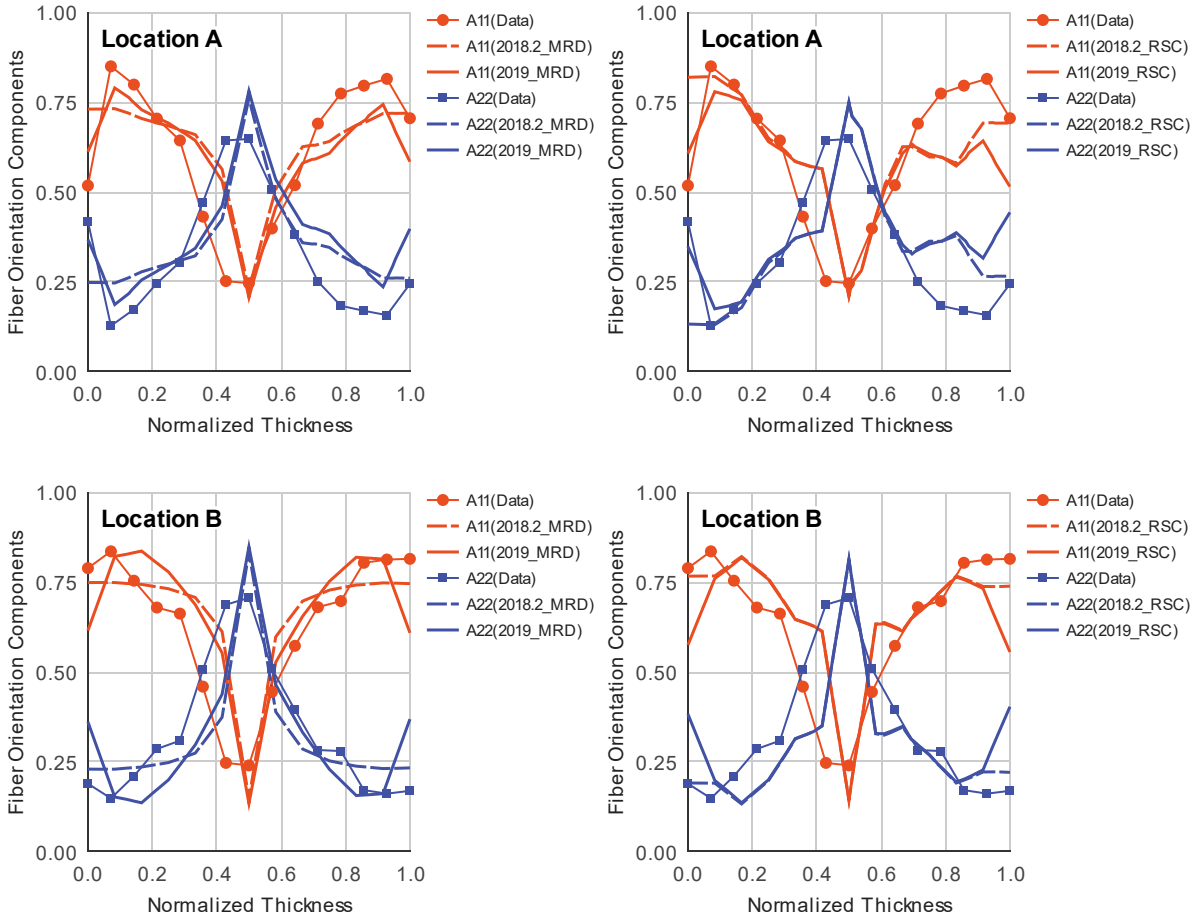

Figure 14. Comparison of fiber orientation data and MRD (left) and RSC (right) predictions by AMI 2018.2 and AMI 2019 in the Delphi ISO-standard plaque of 2 mm thick and fast fill rate.

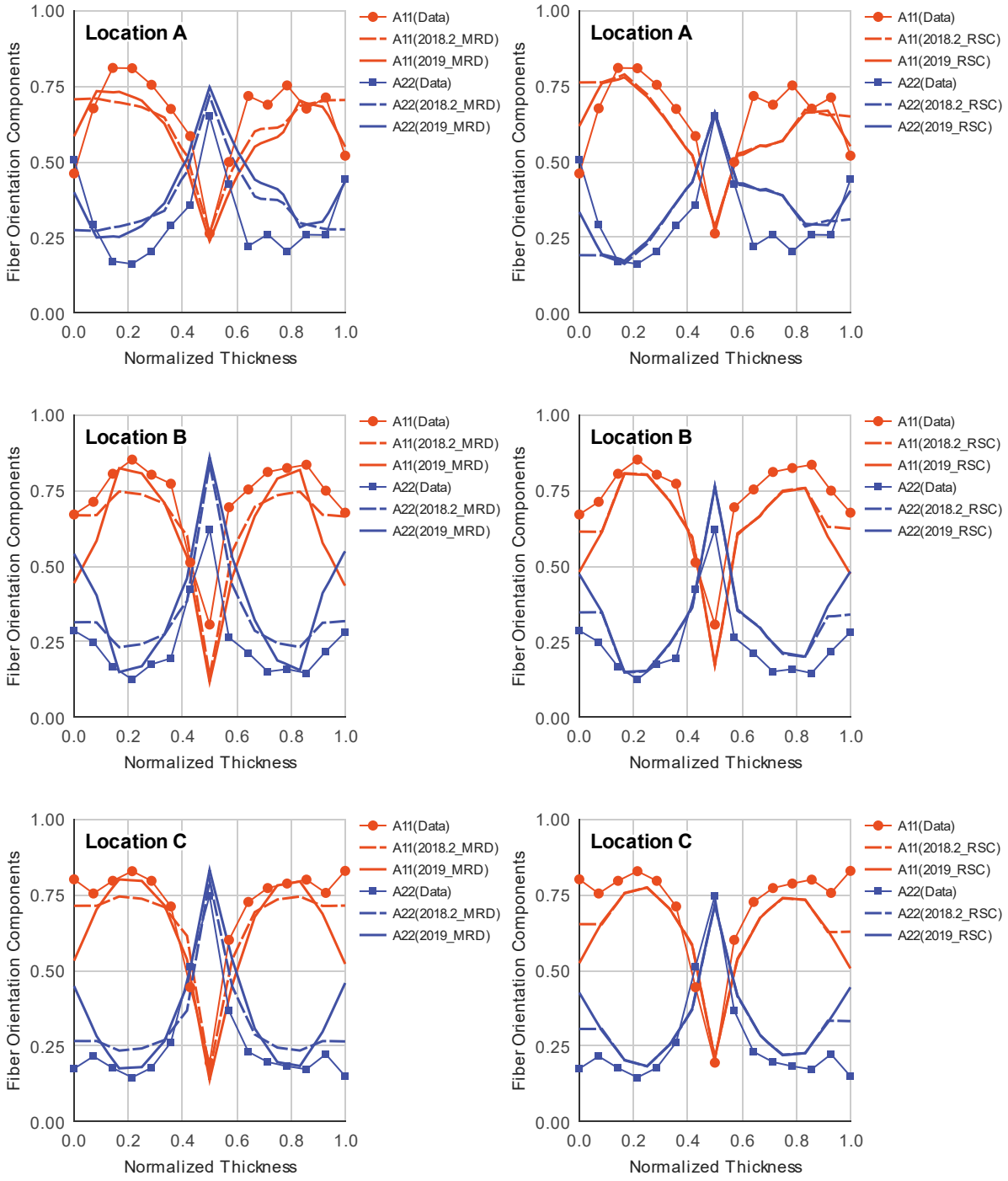

Figure 15. Comparison of fiber orientation data and MRD (left) and RSC (right) predictions by AMI 2018.2 and AMI 2019 in the Delphi ISO-standard plaque of 3 mm thick and slow fill rate.

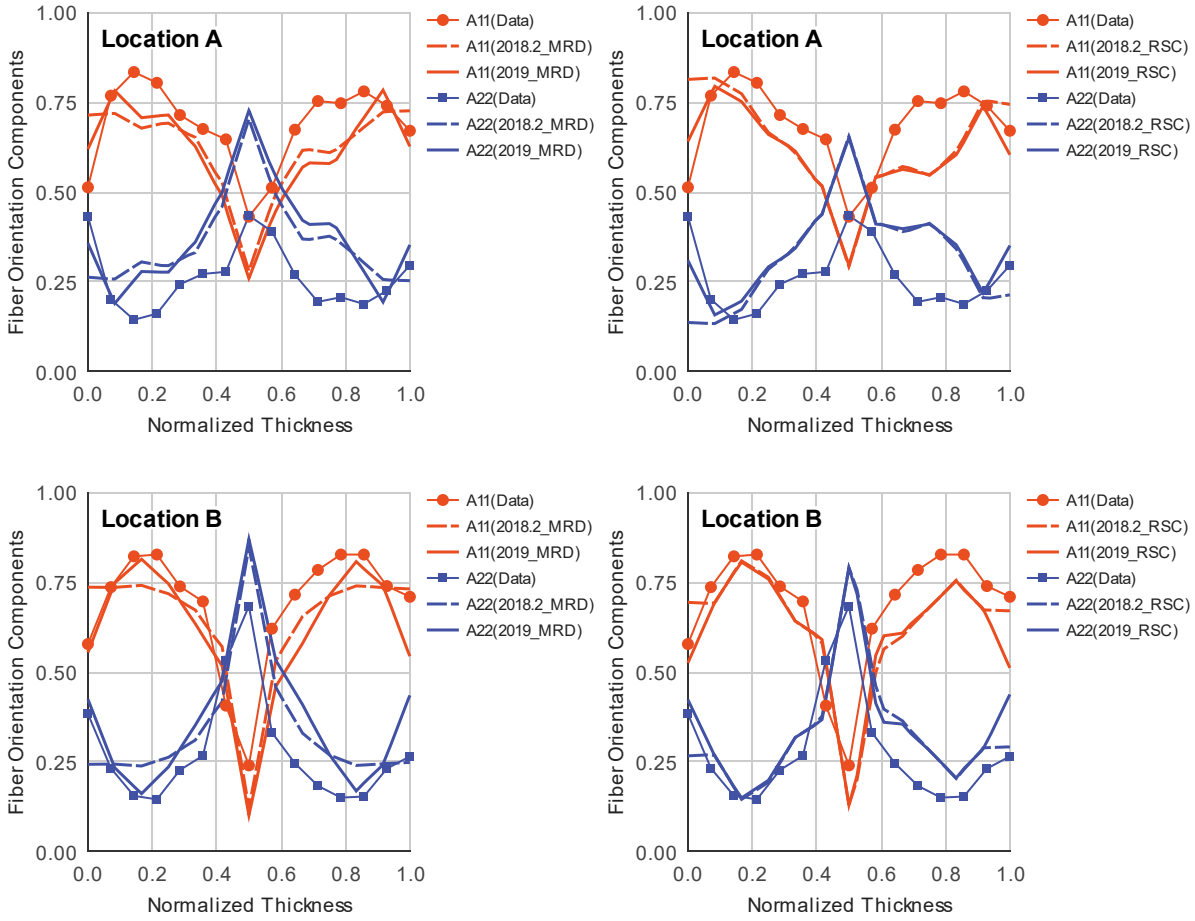

Figure 16. Comparison of fiber orientation data and MRD (left) and RSC (right) predictions by AMI 2018.2 and AMI 2019 in the Delphi ISO-standard plaque of 3 mm thick and medium fill rate.

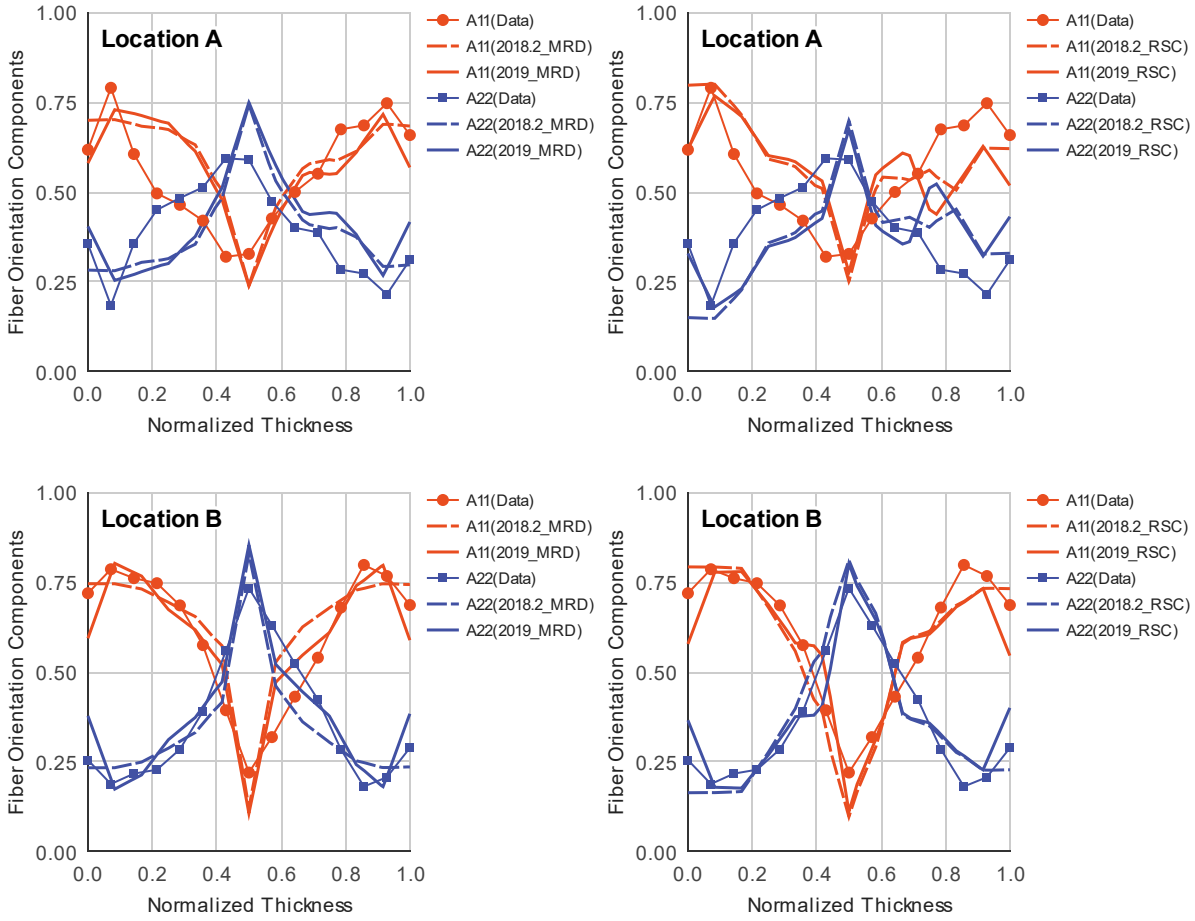

Figure 17. Comparison of fiber orientation data and MRD (left) and RSC (right) predictions by AMI 2018.2 and AMI 2019 in the Delphi ISO-standard plaque of 3 mm thick and fast fill rate.

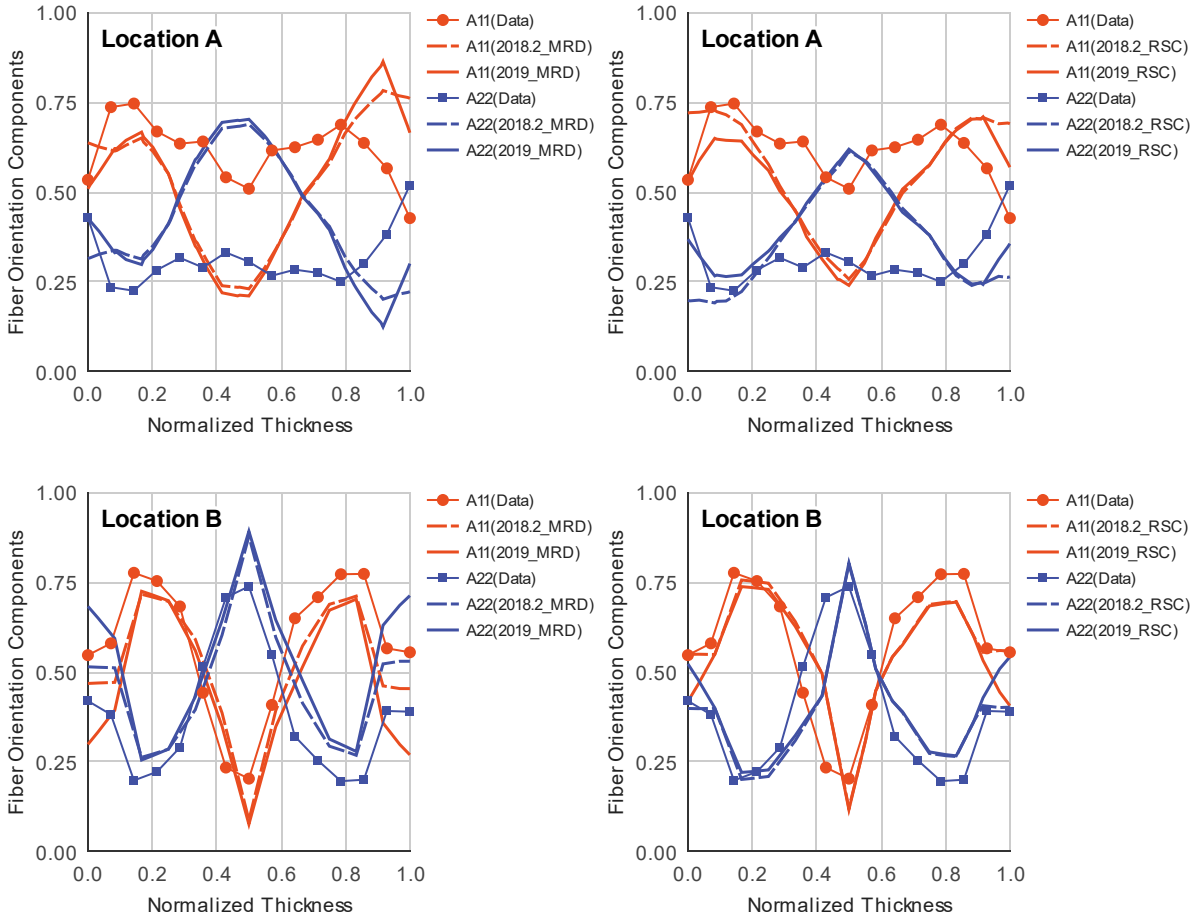

Figure 18. Comparison of fiber orientation data and MRD (left) and RSC (right) predictions by AMI 2018.2 and AMI 2019 in the Delphi ISO-standard plaque of 6 mm thick and slow fill rate.

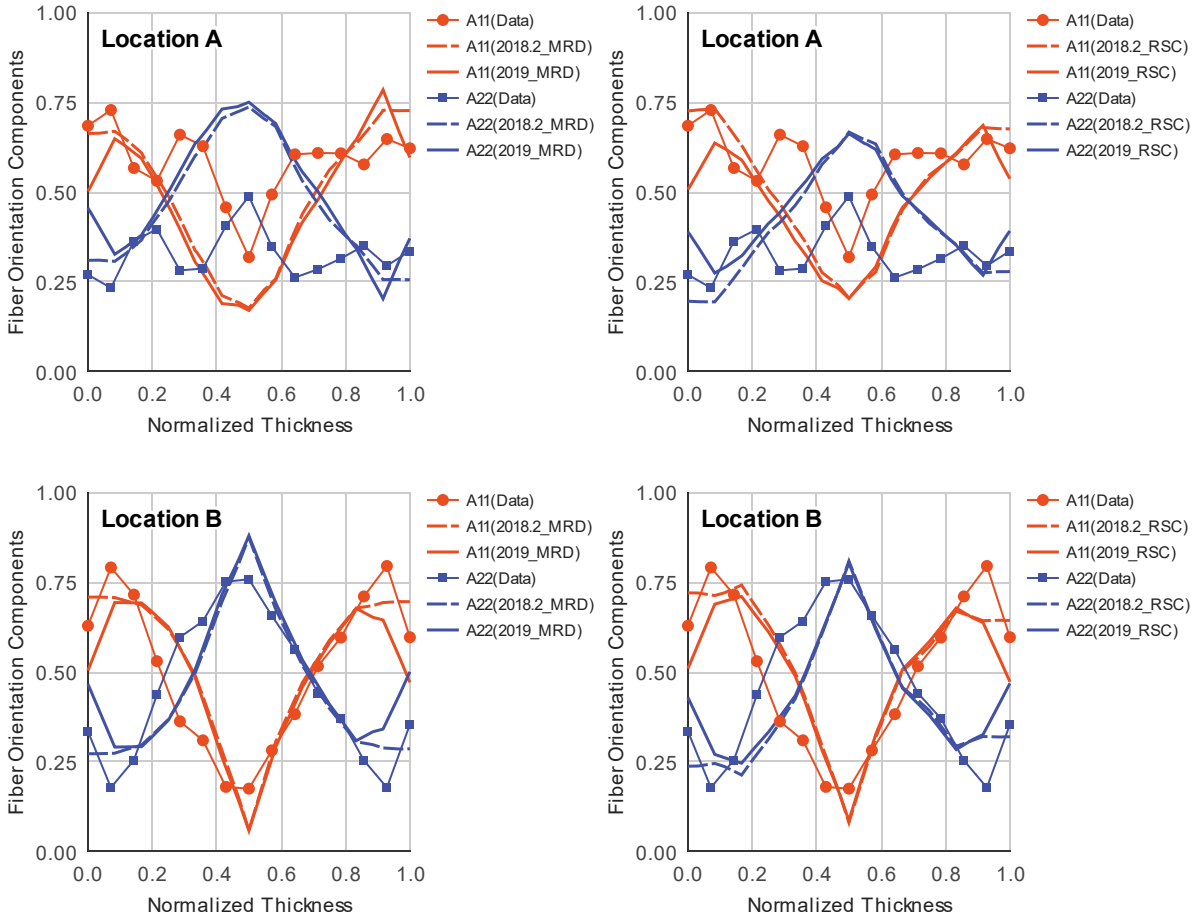

Figure 19. Comparison of fiber orientation data and MRD (left) and RSC (right) predictions by AMI 2018.2 and AMI 2019 in the Delphi ISO-standard plaque of 6 mm thick and medium fill rate.

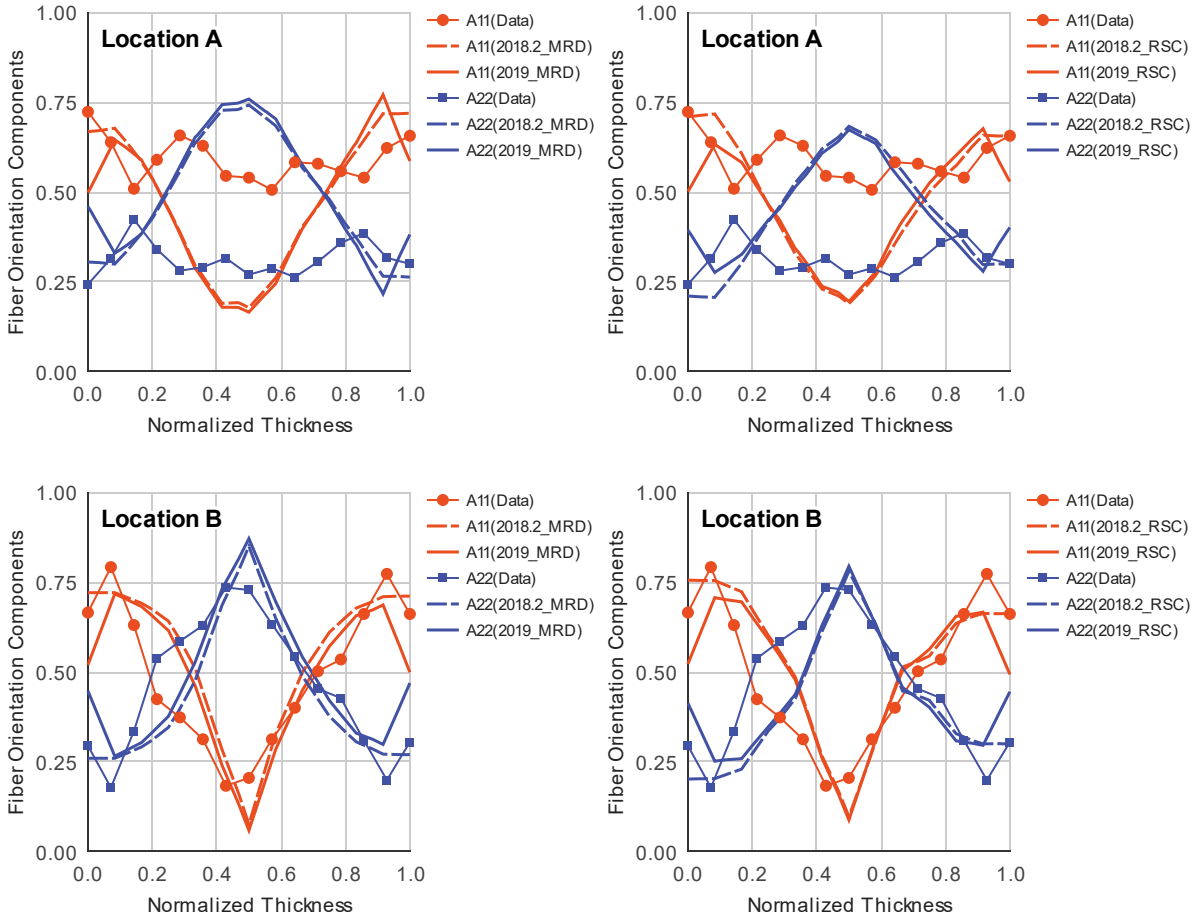

Figure 20. Comparison of fiber orientation data and MRD (left) and RSC (right) predictions by AMI 2018.2 and AMI 2019 in the Delphi ISO-standard plaque of 6 mm thick and fast fill rate.

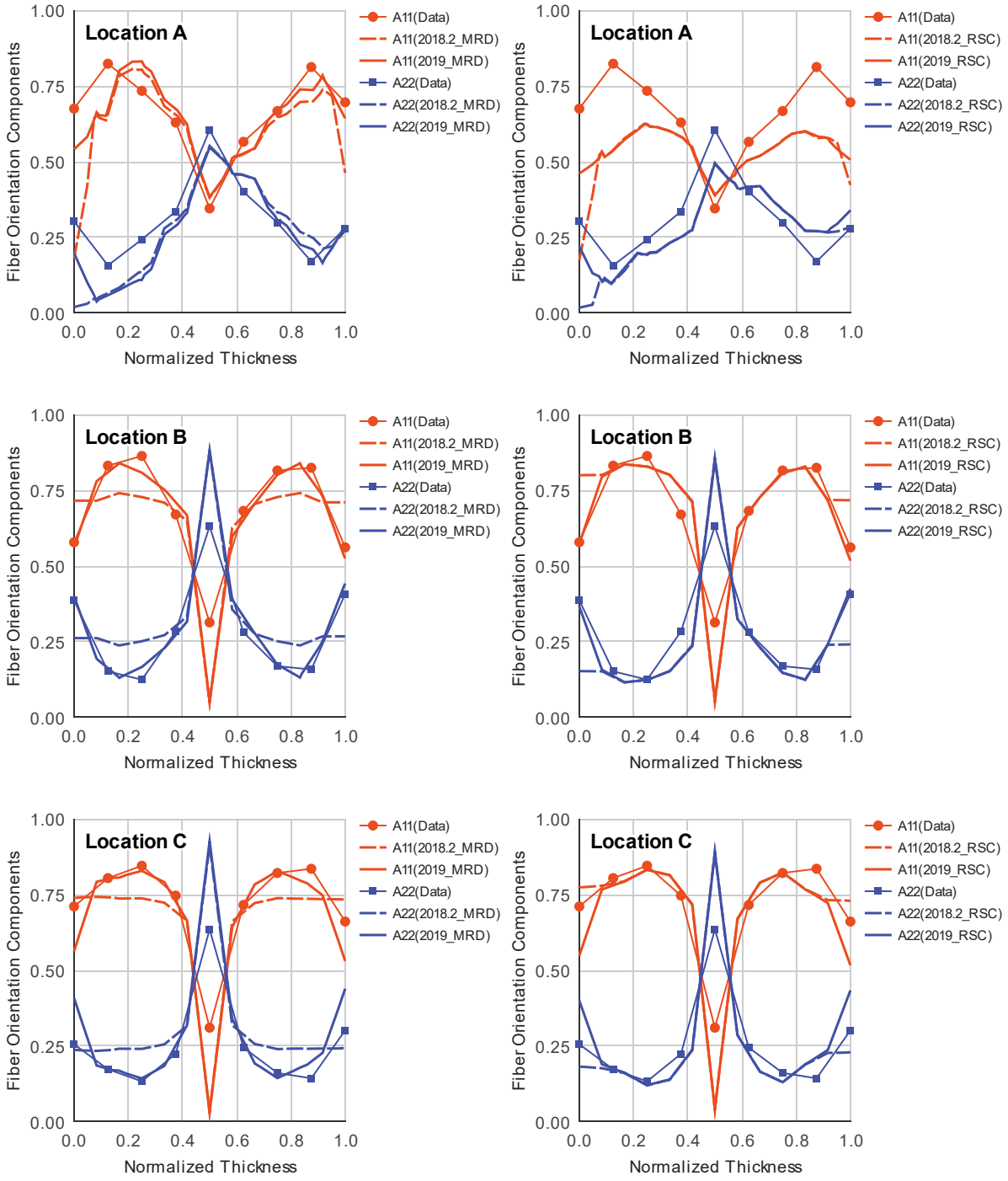

Figure 21. Comparison of fiber orientation data and MRD (left) and RSC (right) predictions by AMI 2018.2 and AMI 2019 in the Delphi disk of 1.5 mm thick and slow fill rate.

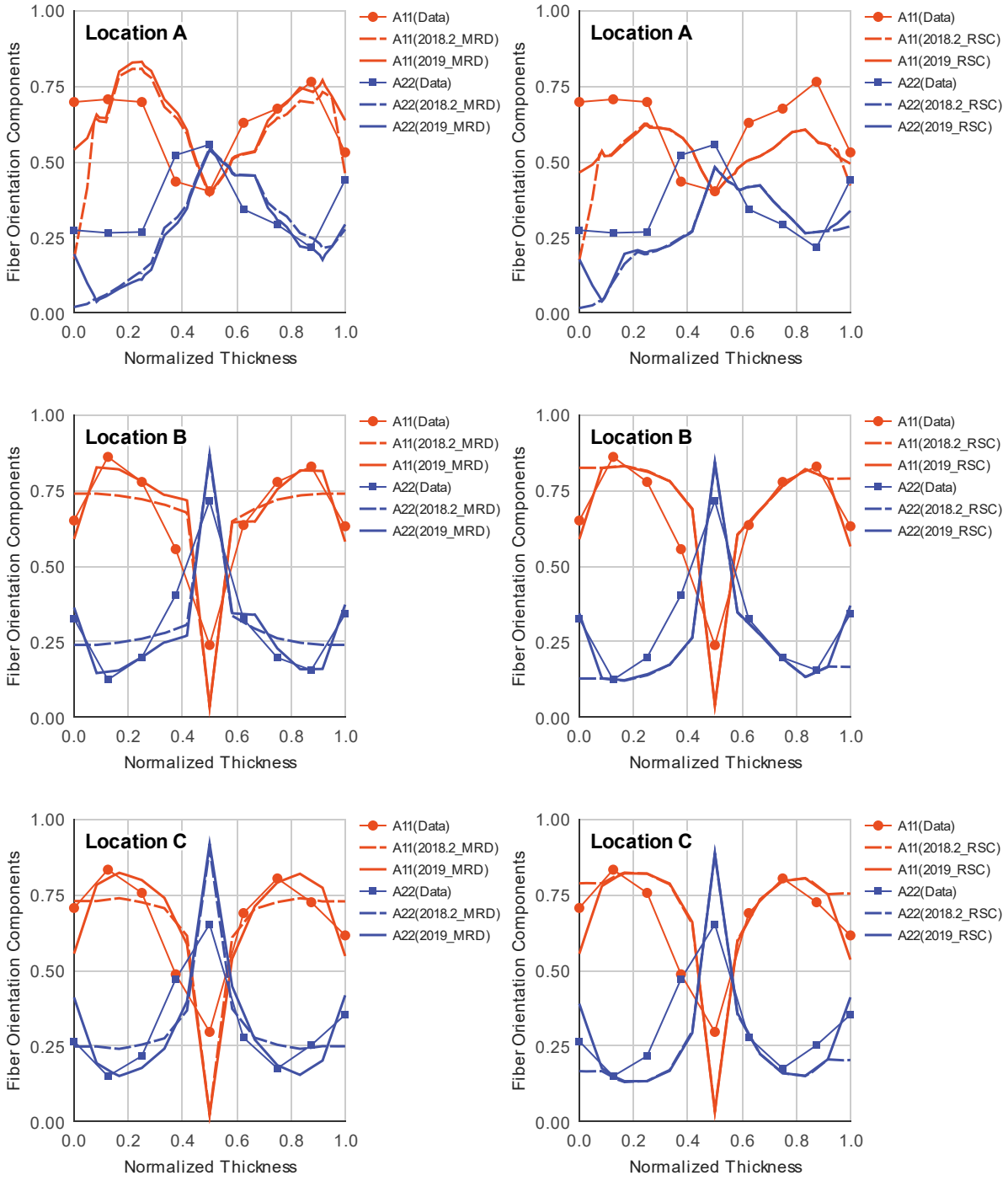

Figure 22. Comparison of fiber orientation data and MRD (left) and RSC (right) predictions by AMI 2018.2 and AMI 2019 in the Delphi disk of 1.5 mm thick and medium fill rate.

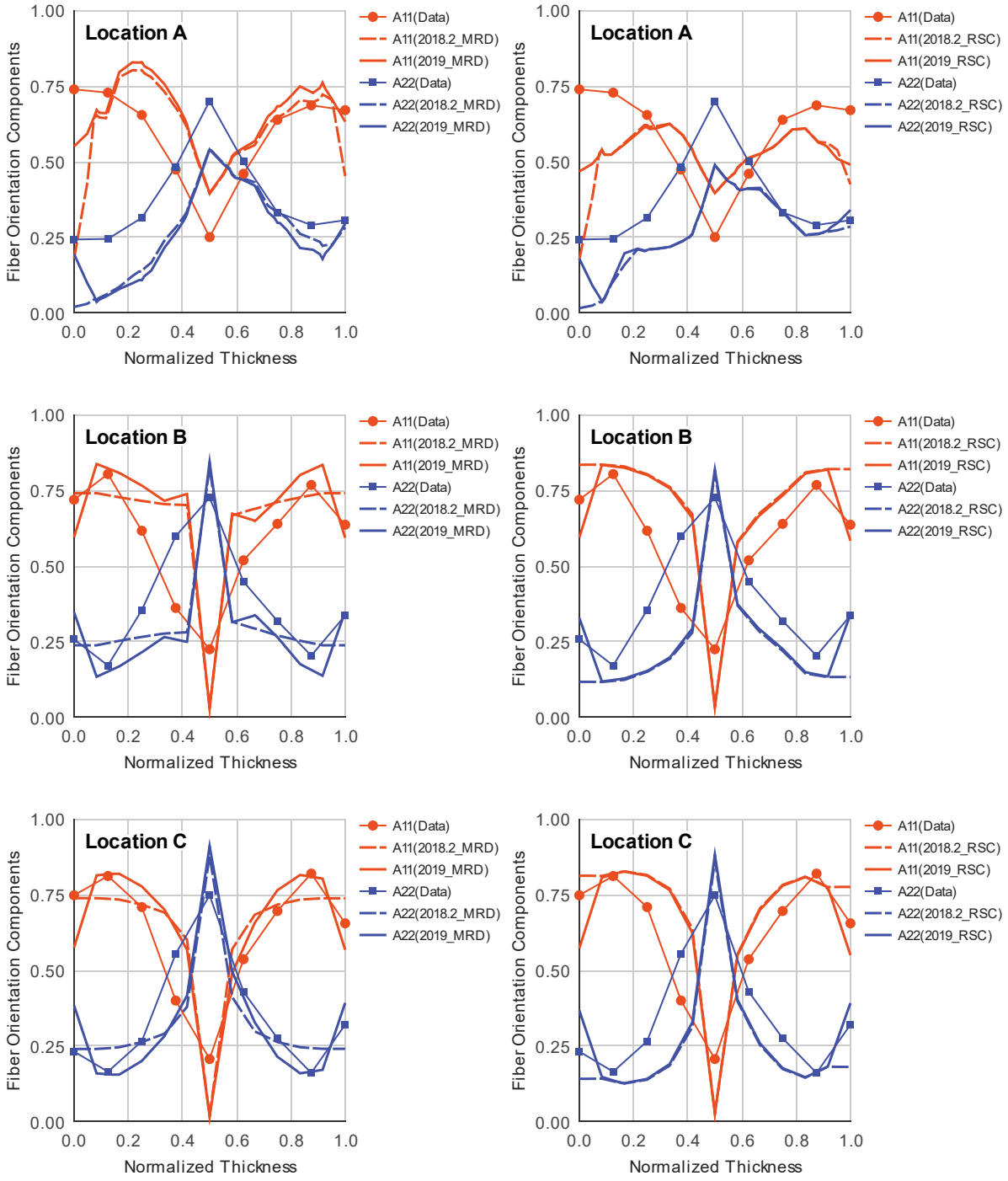

Figure 23. Comparison of fiber orientation data and MRD (left) and RSC (right) predictions by AMI 2018.2 and AMI 2019 in the Delphi disk of 1.5 mm thick and fast fill rate.

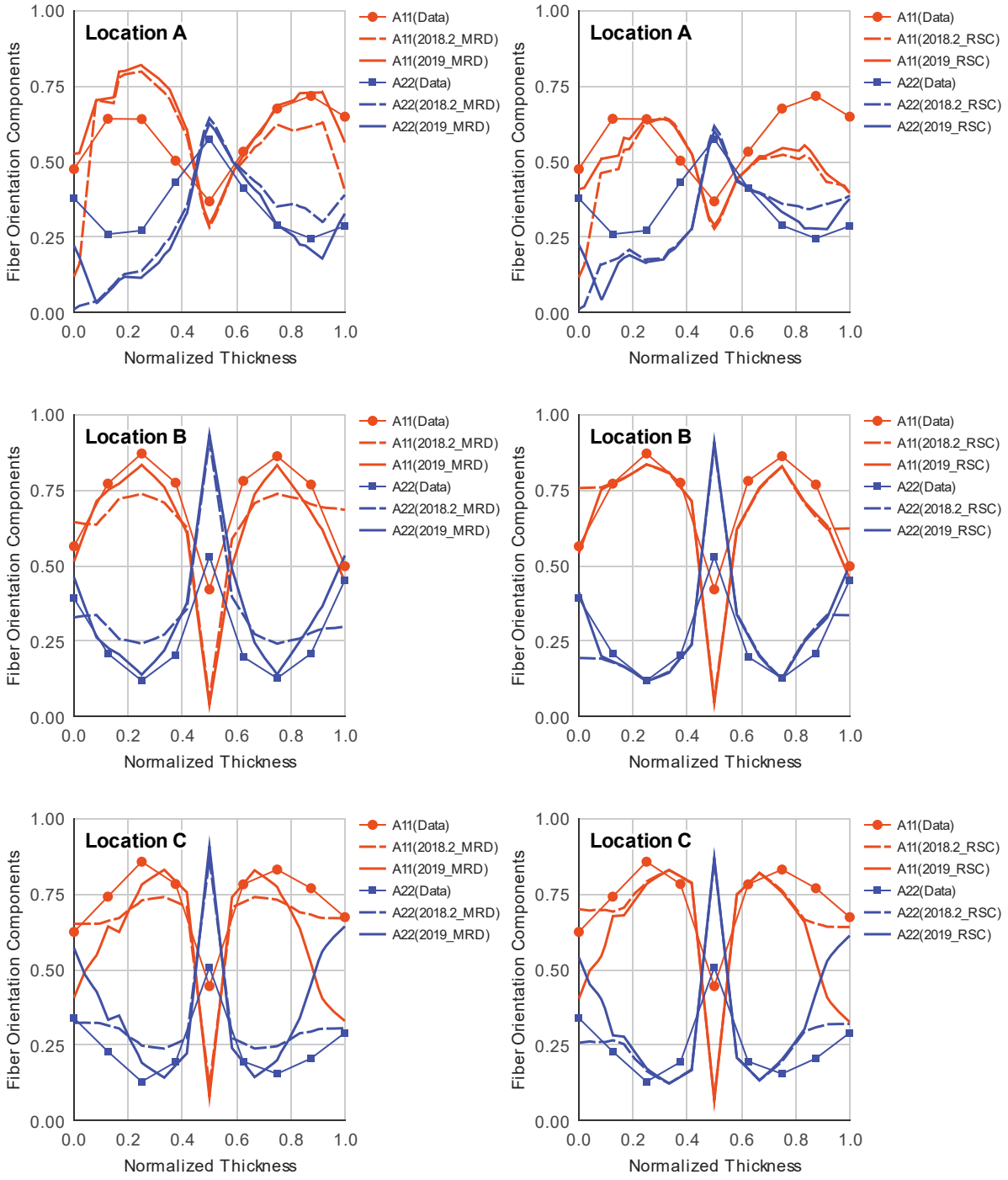

Figure 24. Comparison of fiber orientation data and MRD (left) and RSC (right) predictions by AMI 2018.2 and AMI 2019 in the Delphi disk of 2 mm thick and slow fill rate.

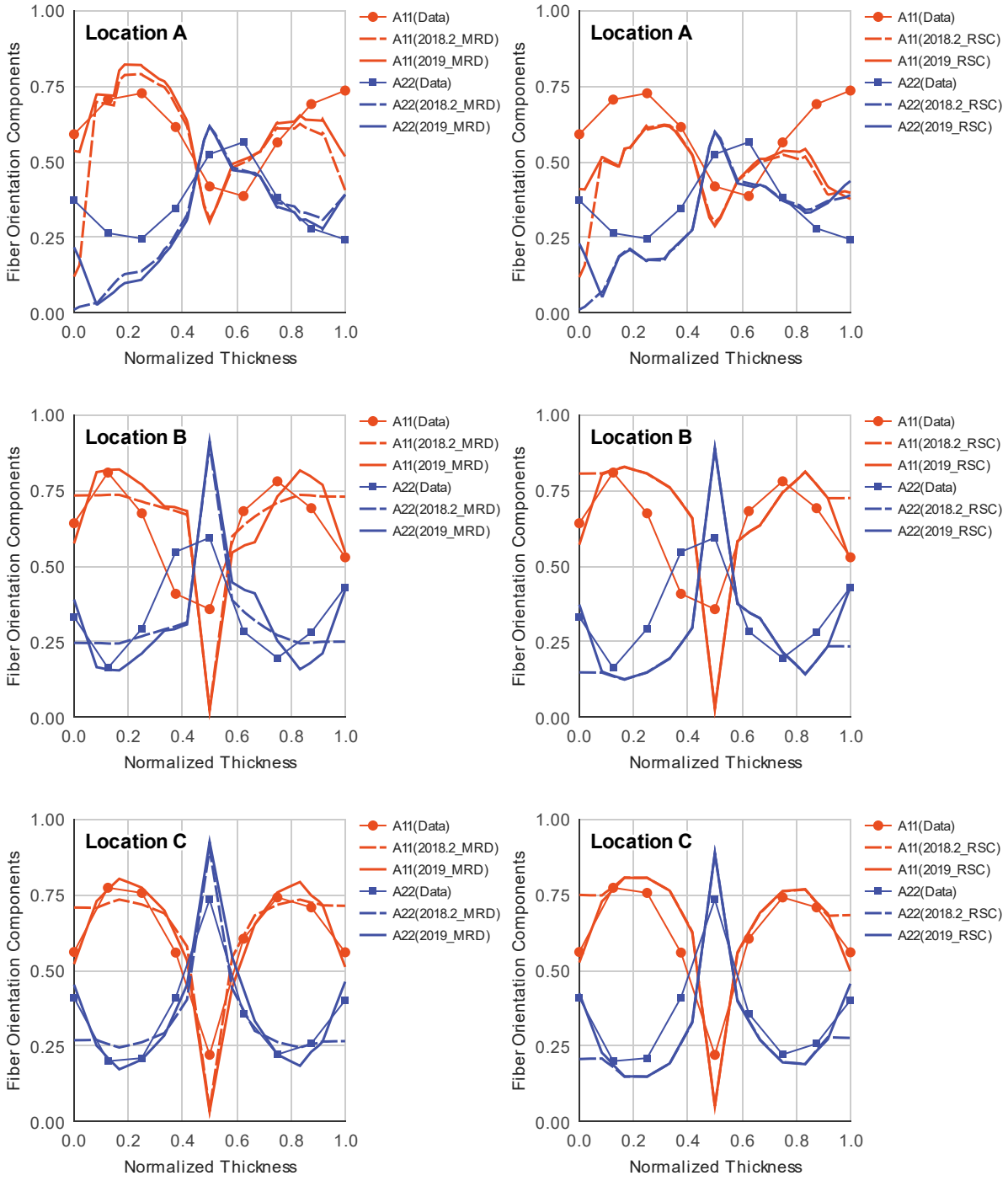

Figure 25. Comparison of fiber orientation data and MRD (left) and RSC (right) predictions by AMI 2018.2 and AMI 2019 in the Delphi disk of 2 mm thick and medium fill rate.

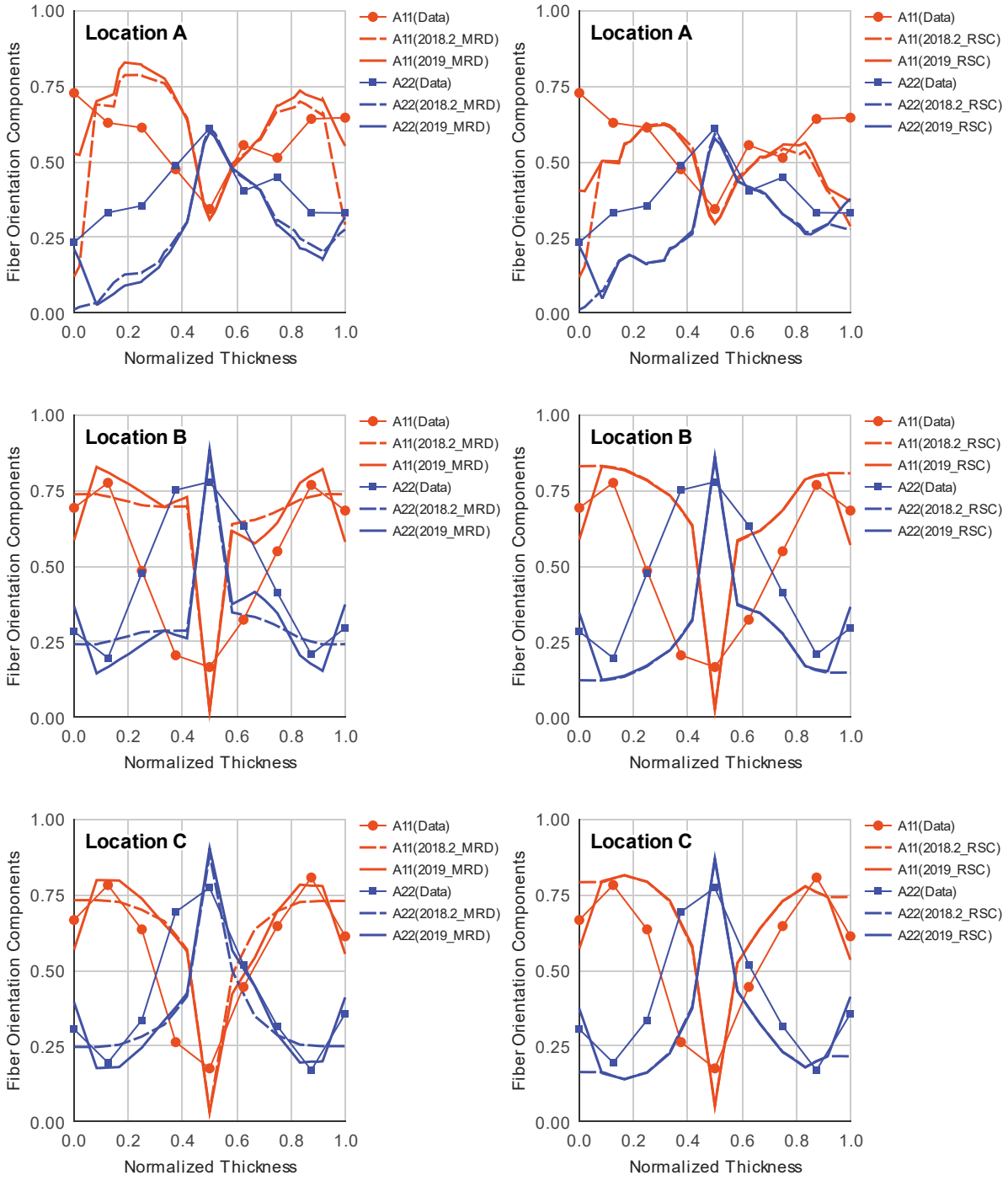

Figure 26. Comparison of fiber orientation data and MRD (left) and RSC (right) predictions by AMI 2018.2 and AMI 2019 in the Delphi disk of 2 mm thick and fast fill rate.

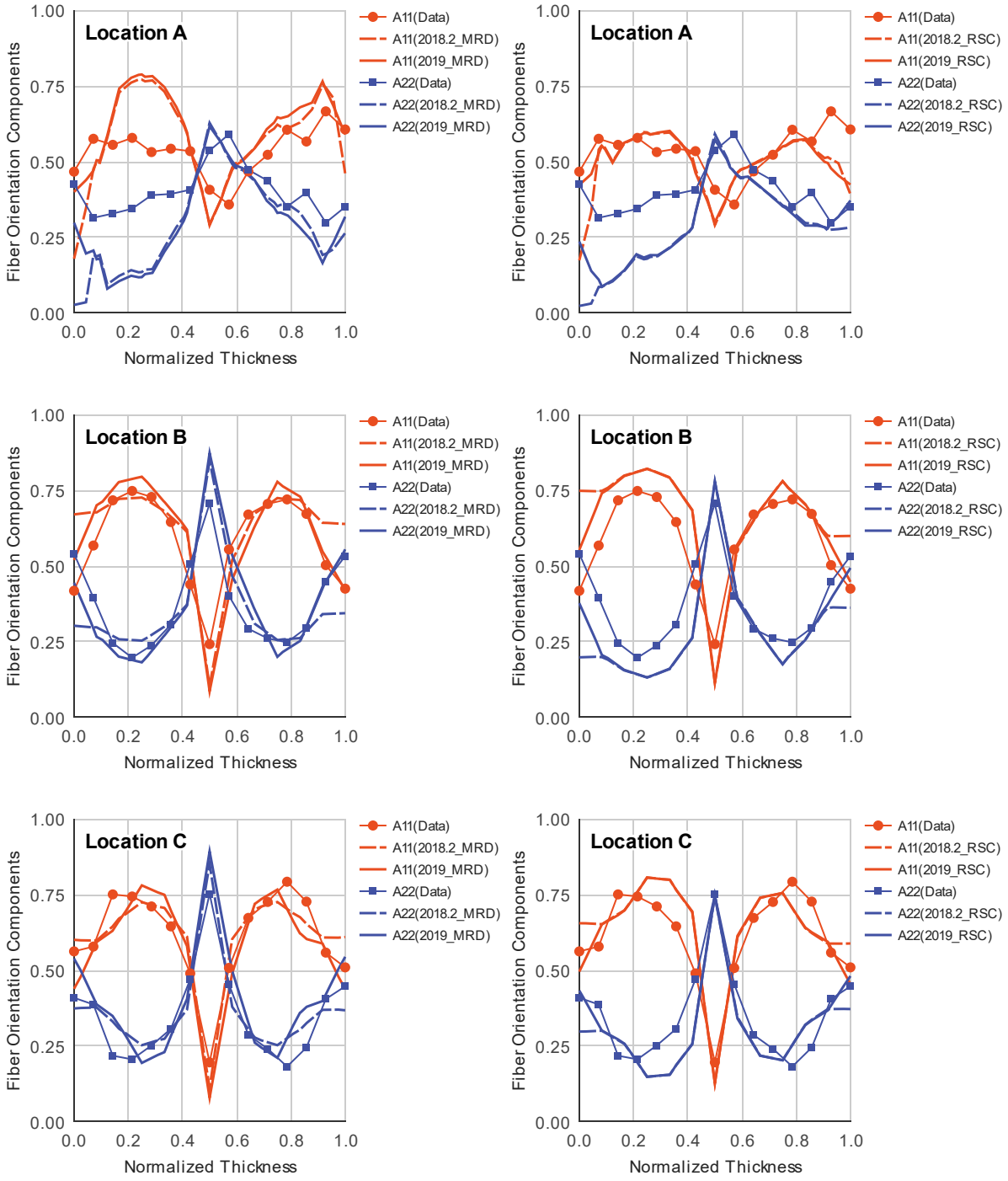

Figure 27. Comparison of fiber orientation data and MRD (left) and RSC (right) predictions by AMI 2018.2 and AMI 2019 in the Delphi disk of 3 mm thick and slow fill rate.

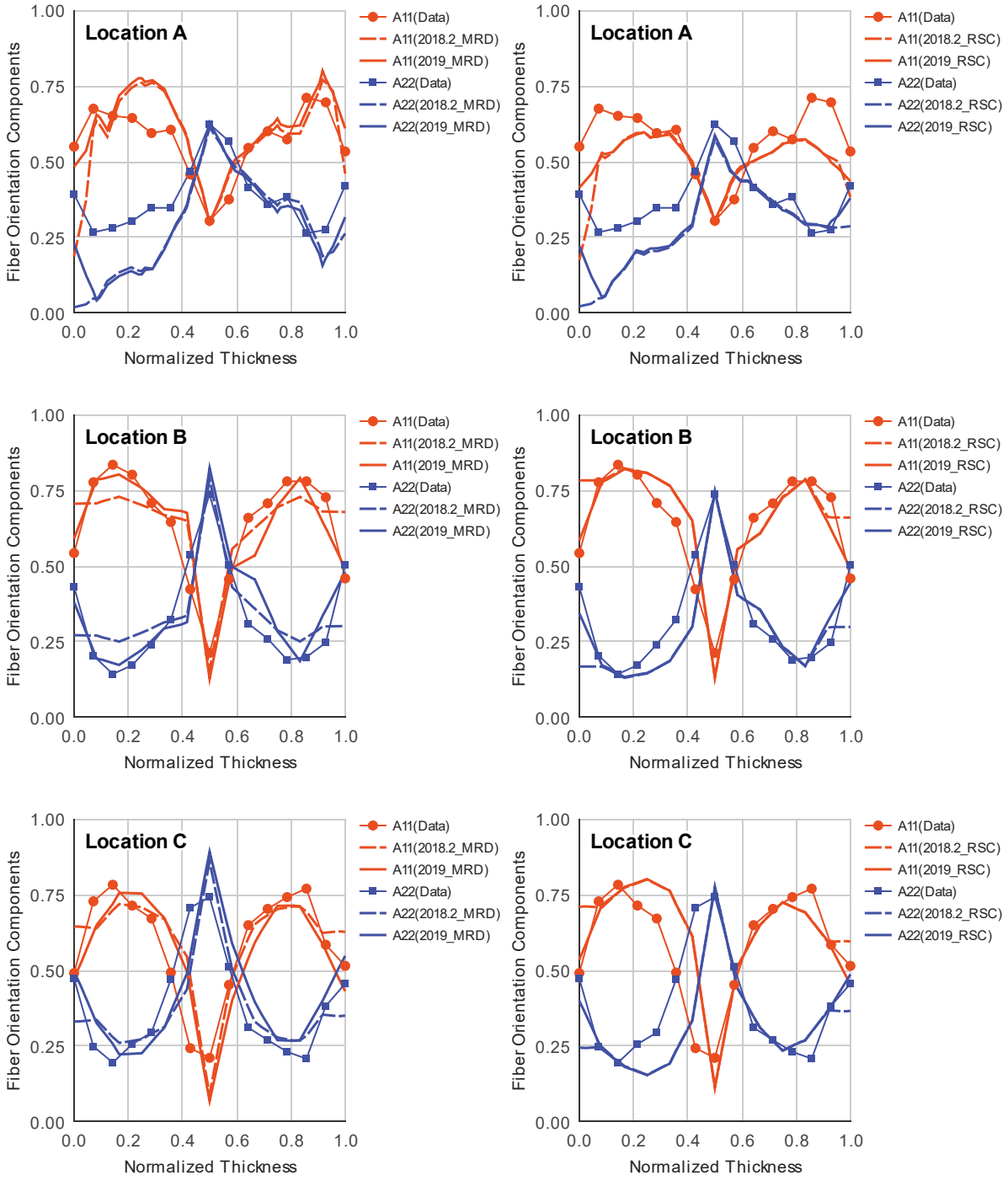

Figure 28. Comparison of fiber orientation data and MRD (left) and RSC (right) predictions by AMI 2018.2 and AMI 2019 in the Delphi disk of 3 mm thick and medium fill rate.

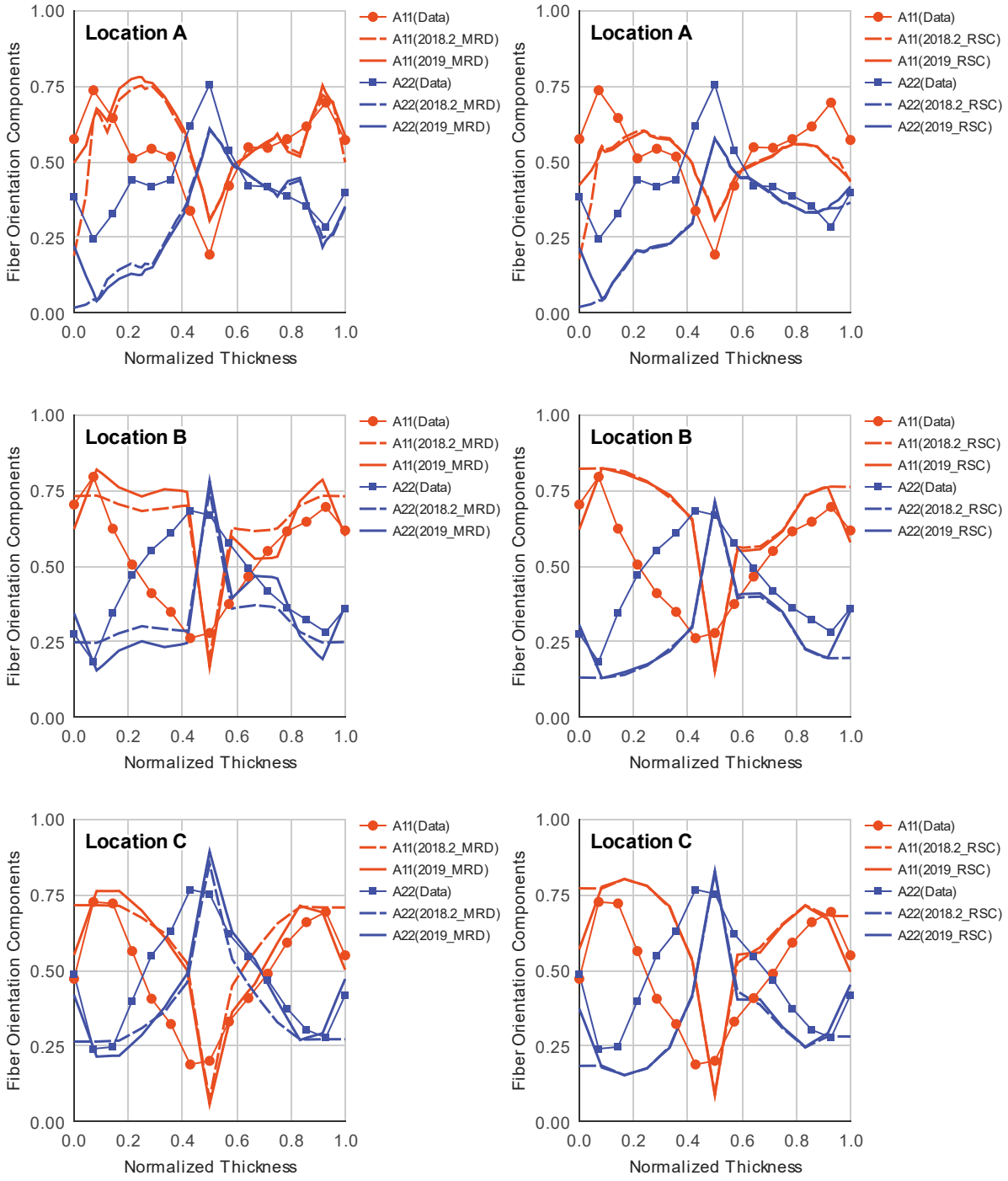

Figure 29. Comparison of fiber orientation data and MRD (left) and RSC (right) predictions by AMI 2018.2 and AMI 2019 in the Delphi disk of 3 mm thick and fast fill rate.

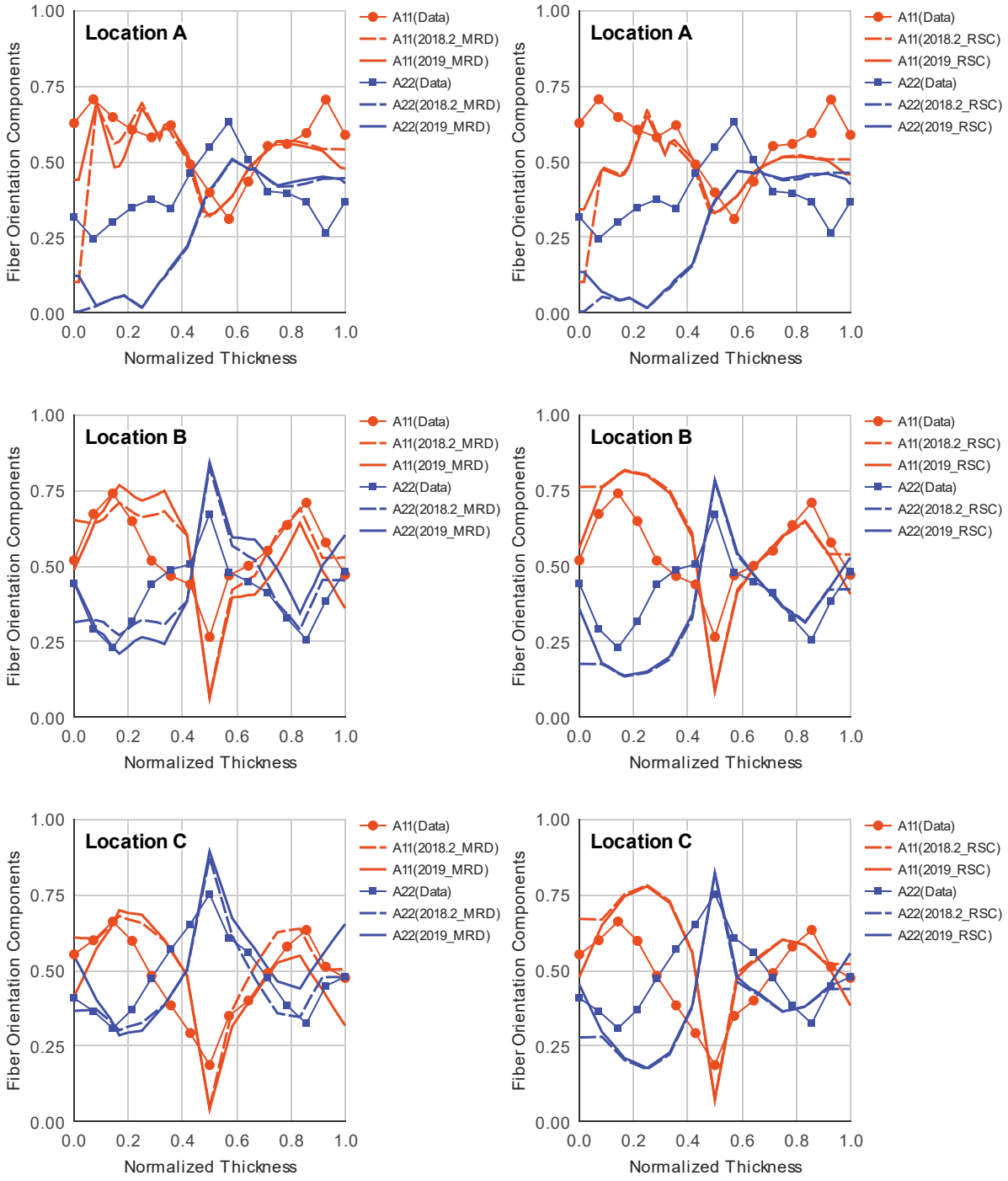

Figure 30. Comparison of fiber orientation data and MRD (left) and RSC (right) predictions by AMI 2018.2 and AMI 2019 in the Delphi disk of 6 mm thick and slow fill rate.

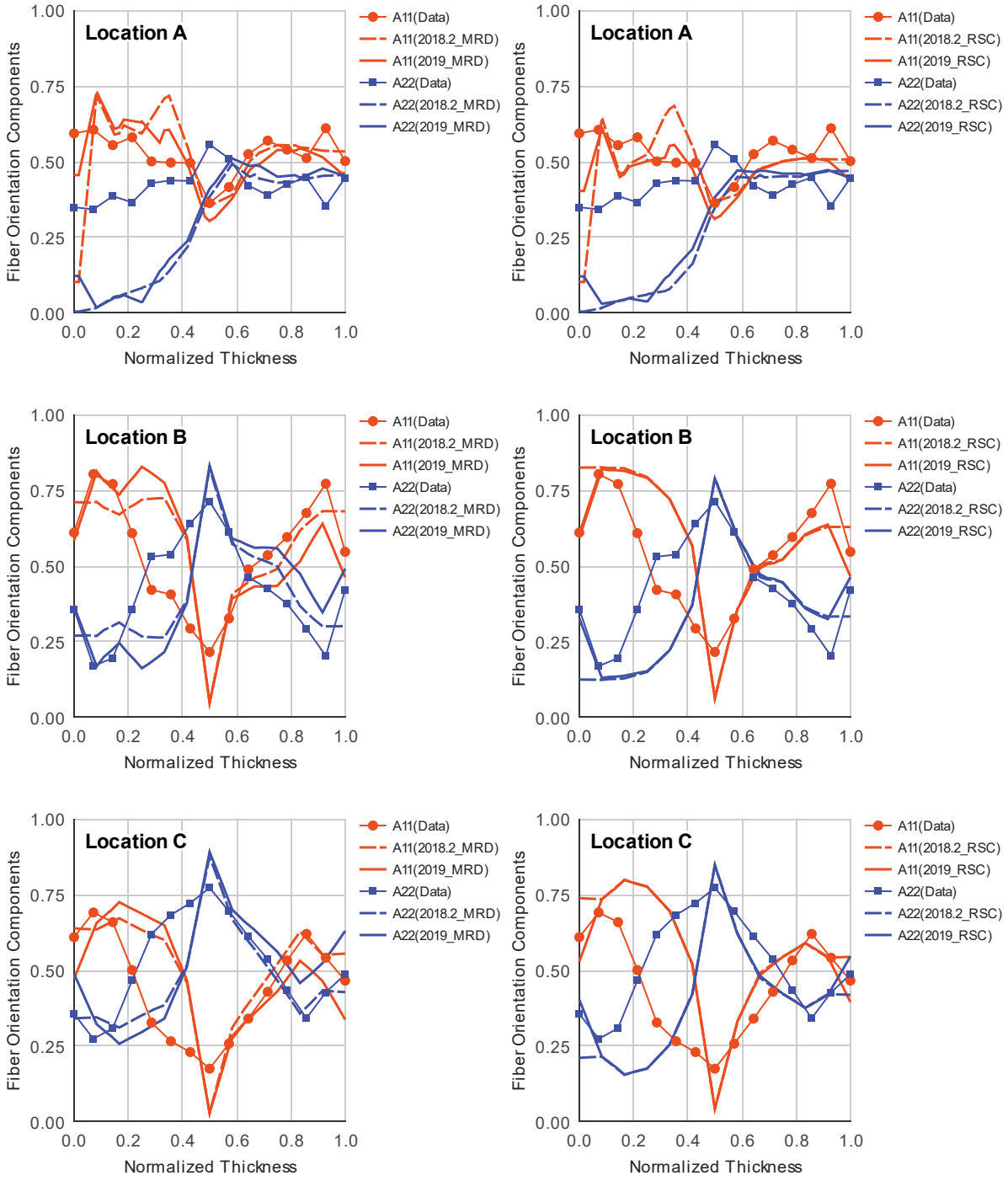

Figure 31. Comparison of fiber orientation data and MRD (left) and RSC (right) predictions by AMI 2018.2 and AMI 2019 in the Delphi disk of 6 mm thick and medium fill rate.

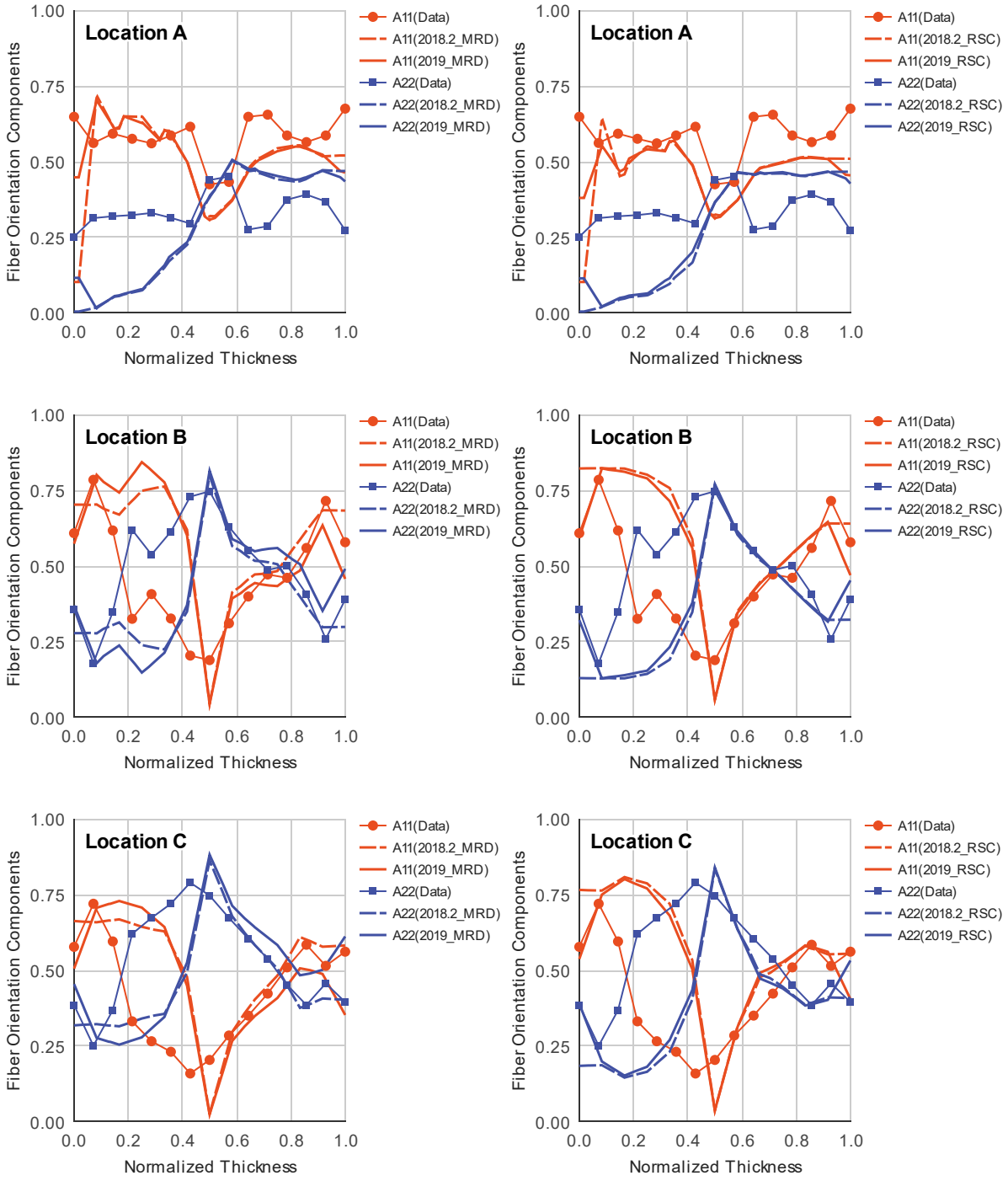

Figure 32. Comparison of fiber orientation data and MRD (left) and RSC (right) predictions by AMI 2018.2 and AMI 2019 in the Delphi disk of 6 mm thick and fast fill rate.

Bradford inverted cup

An inverted cup was molded from Rhodia Engineering Plastics Technyl C 216 V40 Natural (40 wt% short fiber-reinforced polyamide) by Bradford University. The diameter of the cup is 95 mm and the height is 27.8 mm. The fiber orientation was measured at three locations which are 16.5, 25.15, and 36.5 mm away from the center runner, respectively, and are labeled as A, B, and C. The geometry, mesh, and measurement locations are illustrated in Figure 33.

The fiber orientation predictions using the MRD and RSC models in AMI 2018.2 and AMI 2019 are compared with the experimental data in Figure 34. The MRD model in AMI 2019 produces better match to shell orientation than in AMI 2018.2. AMI 2019 matches the skin orientation than AMI 2018.2 for both the MRD and RSC models.

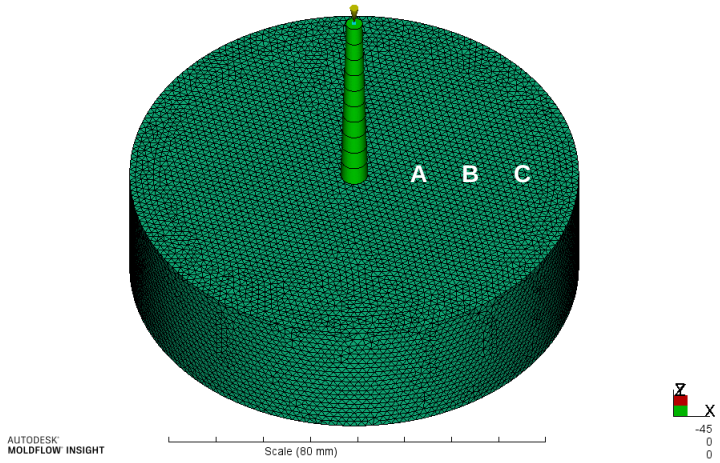

Figure 33. Geometry, 3D mesh, and locations of measurement samples for Bradford inverted cup.

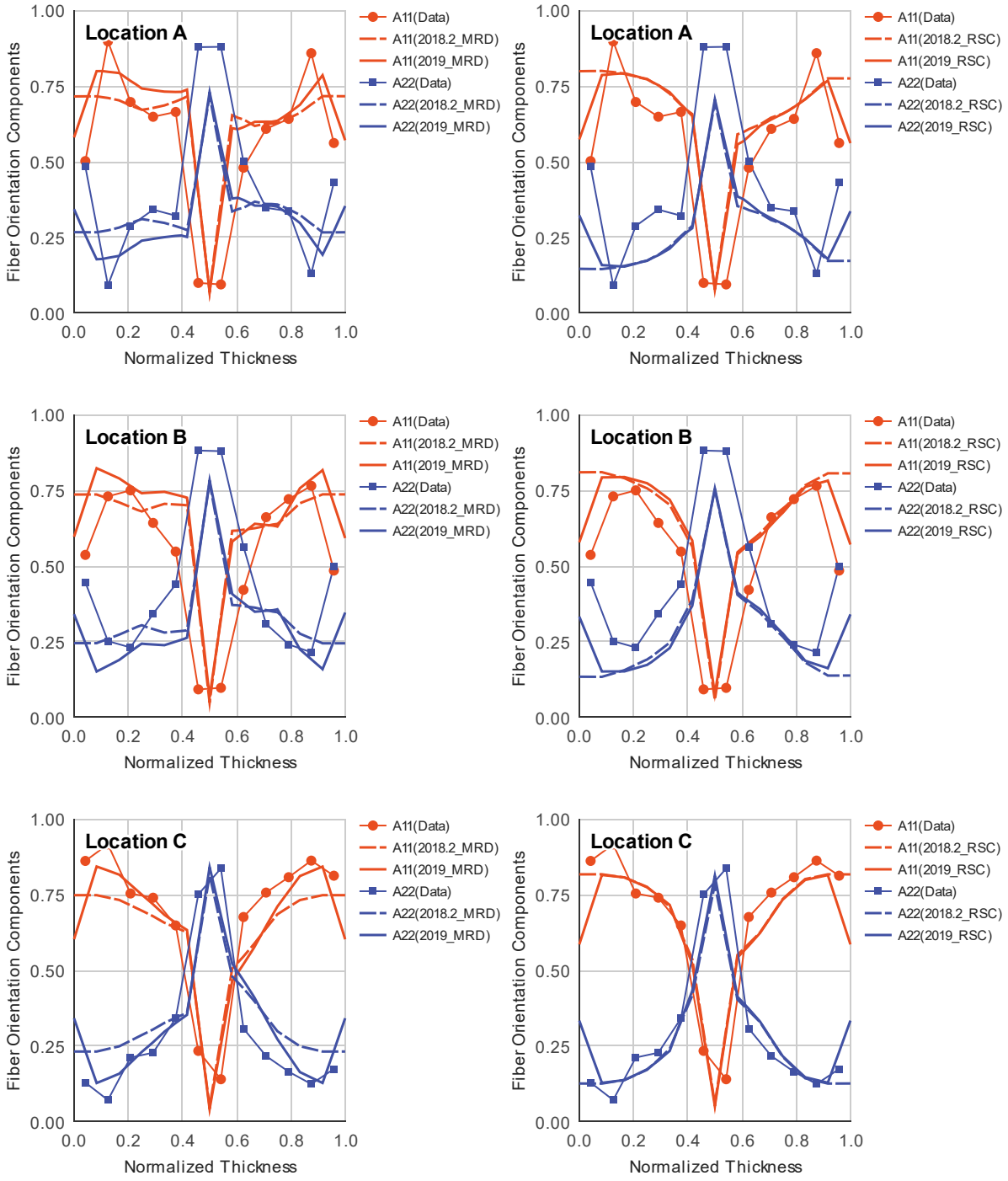

Figure 34. Comparison of fiber orientation data and MRD (left) and RSC (right) predictions by AMI 2018.2 and AMI 2019 in the Bradford inverted cup.

DSM plaque

A plaque was molded from DSM Akulon K224-PG8 (40 wt% glass fiber-reinforced PA6) by DSM. The dimension of the plaque is 270 mm long, 310 mm wide, and 2 mm thick. The fiber orientation was measured at six locations. Locations 1, 2, and 3 are along the centerline, and 200, 100, and 30 mm away from the end of the plaque, respectively. Locations 6, 5, and 4 are 80 mm away from the centerline, and 200, 100, and 30 mm away from the end of the plaque, respectively. The geometry, mesh, and measurement locations are illustrated in Figure 35.

The fiber orientation predictions using the MRD and RSC models in AMI 2018.2 and AMI 2019 are compared with the experimental data in Figure 36. The fiber orientation predictions in AMI 2019 show good agreement with the experimental data and are also better than in AMI 2018.2.

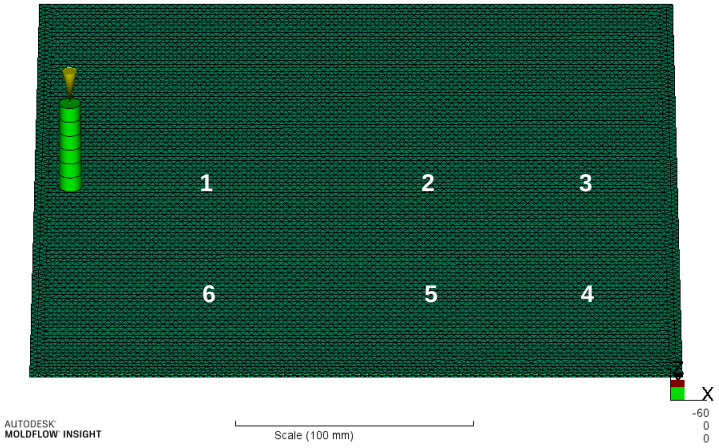

Figure 35. Geometry, 3D mesh, and locations of measurement samples for DSM plaque.

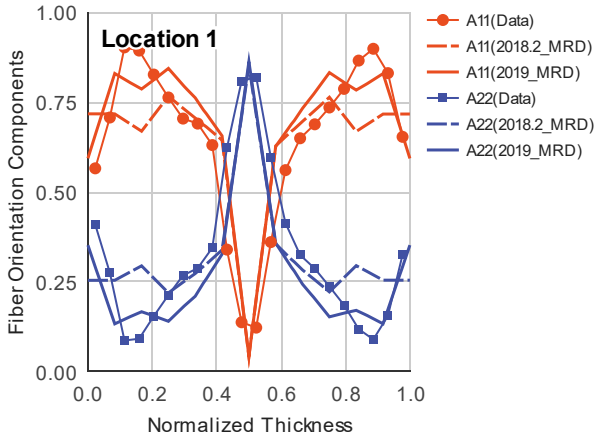
Location 1
Fiber Orientation Components
Normalized Thickness
1.00
0.75
0.50
0.25
0.00
0.0
0.2
0.4
0.6
0.8
1.0
A11(Data)
A11(2018.2_MRD)
A11(2019_MRD)
A22(Data)
A22(2018.2_MRD)
A22(2019_MRD)

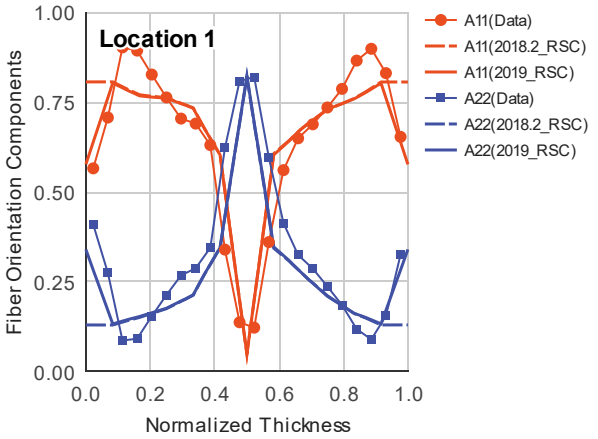
Location 1
Fiber Orientation Components
Normalized Thickness
1.00
0.75
0.50
0.25
0.00
0.0
0.2
0.4
0.6
0.8
1.0
A11(Data)
A11(2018.2_RSC)
A11(2019_RSC)
A22(Data)
A22(2018.2_RSC)
A22(2019_RSC)

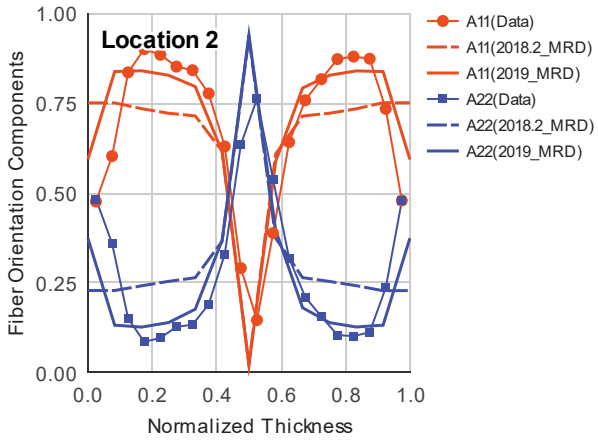
Location 2
Fiber Orientation Components
Normalized Thickness
1.00
0.75
0.50
0.25
0.00
0.0
0.2
0.4
0.6
0.8
1.0
A11(Data)
A11(2018.2_MRD)
A11(2019_MRD)
A22(Data)
A22(2018.2_MRD)
A22(2019_MRD)

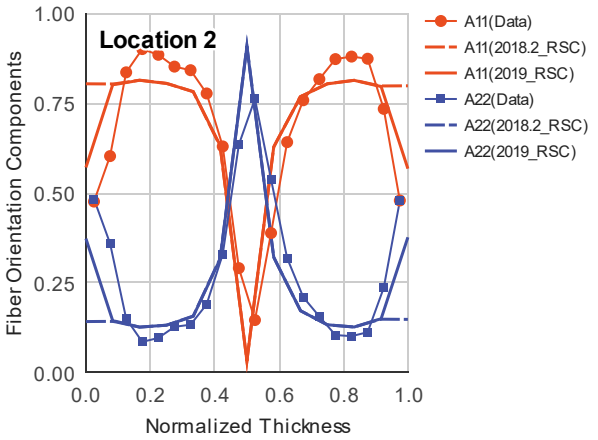
Location 2
Fiber Orientation Components
Normalized Thickness
1.00
0.75
0.50
0.25
0.00
0.0
0.2
0.4
0.6
0.8
1.0
A11(Data)
A11(2018.2_RSC)
A11(2019_RSC)
A22(Data)
A22(2018.2_RSC)
A22(2019_RSC)

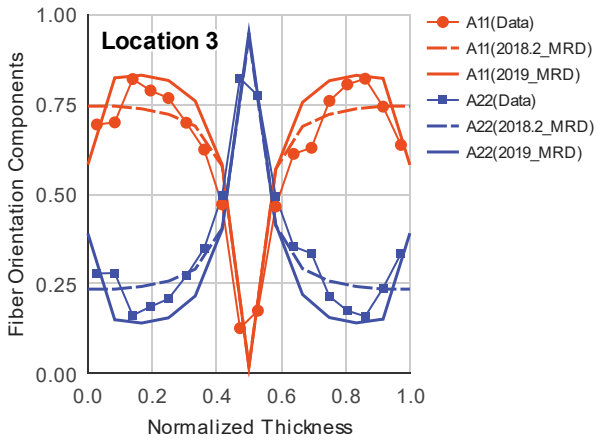
Location 3
Fiber Orientation Components
Normalized Thickness
1.00
0.75
0.50
0.25
0.00
0.0
0.2
0.4
0.6
0.8
1.0
A11(Data)
A11(2018.2_MRD)
A11(2019_MRD)
A22(Data)
A22(2018.2_MRD)
A22(2019_MRD)

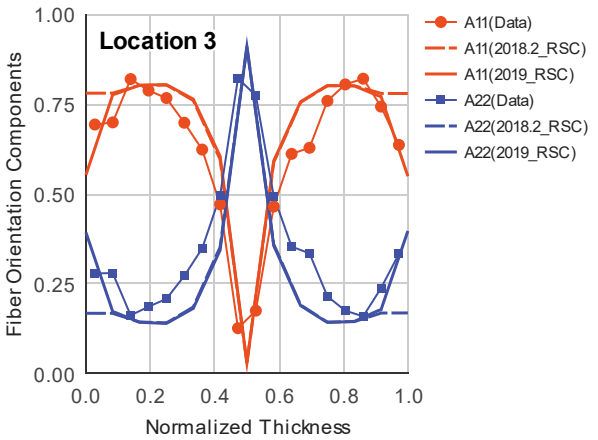
Location 3
Fiber Orientation Components
Normalized Thickness
1.00
0.75
0.50
0.25
0.00
0.0
0.2
0.4
0.6
0.8
1.0
A11(Data)
A11(2018.2_RSC)
A11(2019_RSC)
A22(Data)
A22(2018.2_RSC)
A22(2019_RSC)

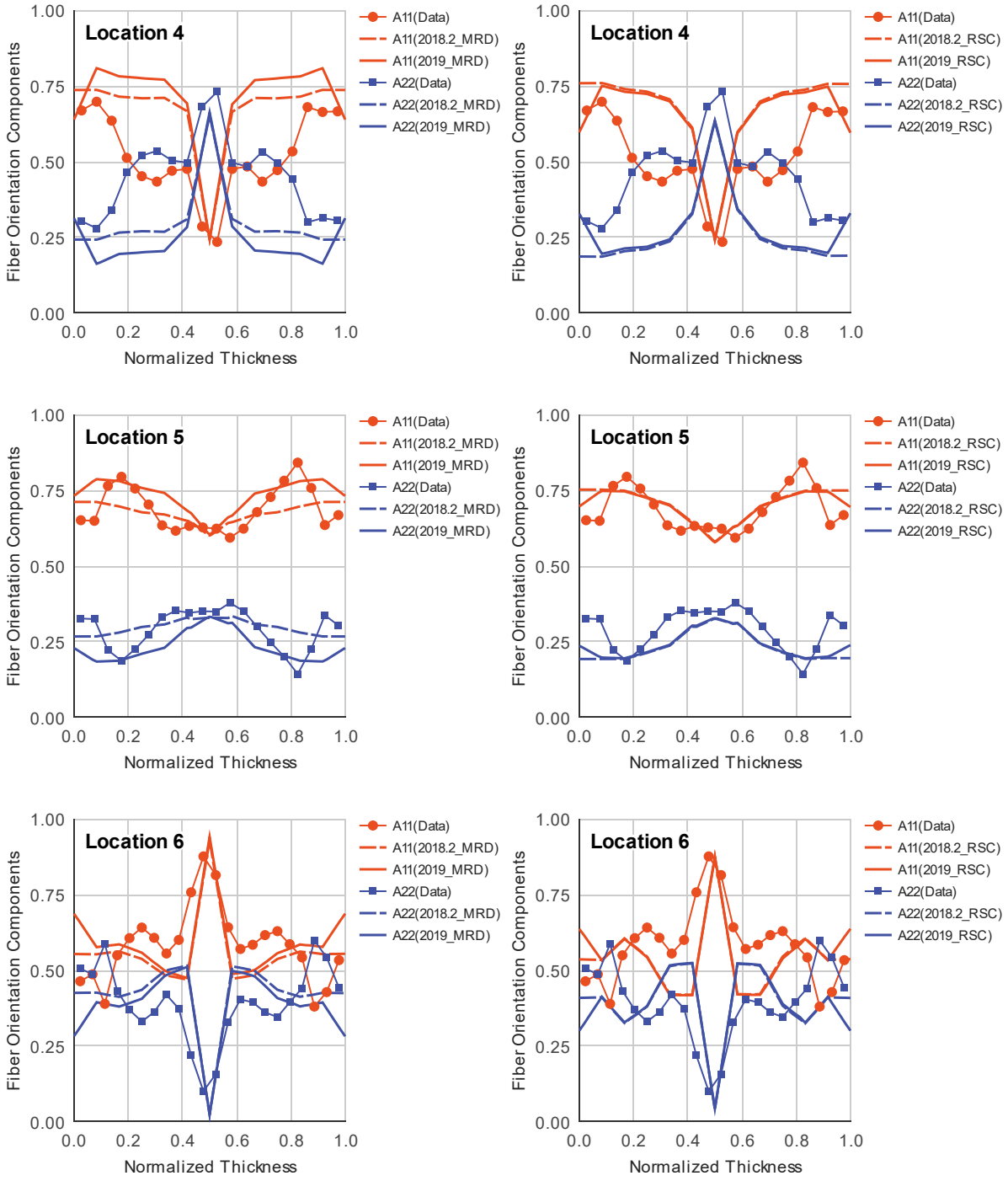

Figure 36. Comparison of fiber orientation data and MRD (left) and RSC (right) predictions by AMI 2018.2 and AMI 2019 in the DSM plaque.

Acknowledgements

Autodesk, Inc. wishes to thank Delphi Automotive LLP, Bradford University, and DSM Engineering Plastics for providing experimental measurements and models of their molded parts, which were used in this report.

References

[1] Bay, R. S., & Tucker III, C. L. (1992). Fiber orientation in simple injection moldings. Part I: Theory and numerical methods. *Polymer Composites*, 13(4), 317–331. http://doi.org/10.1002/pc.750130409

[2] Wang, J., Silva, C. A., Viana, J. C., van Hattum, F. W. J., Cunha, A. M., & Tucker III, C. L. (2008). Prediction of fiber orientation in a rotating compressing and expanding mold. *Polymer Engineering & Science*, 48(7), 1405–1413. http://doi.org/10.1002/pen.20979

[3] Wang, J., O'Gara, J. F., & Tucker III, C. L. (2008). An objective model for slow orientation kinetics in concentrated fiber suspensions: Theory and rheological evidence. Journal of Rheology, 52(5), 1179–1200. http://doi.org/10.1122/1.2946437